REVIEW

DOI: 10.61558/2993-074X.3459 **Article ID:** 1006-3471(2024)00-0000-00

Http://electrochem.xmu.edu.cn

Series Reports (1/4): Advancements in Electrochemical Energy Conversions at Prof Wei's Group of Chongqing University: High-Performance Oxygen Reduction Catalysts for Fuel Cells

Fadong Chen[#], Zhuoyang, Xie[#], Mengting Li, Siguo Chen, Wei Ding, Li Li*, Jing Li*, and Zidong Wei*

State Key Laboratory of Advanced Chemical Power Sources (Chongqing University); The College of Chemistry and Chemical Engineering, Chongqing University, Chongqing, 400044, China

Corresponding Authors: liliracial@cqu.edu.cn; lijing@cqu.edu.cn; and zdwei@cqu.edu.cn

Keywords: Fuel cells; Oxygen reduction reaction; Pt-based catalysts; Carbon-based catalysts

Abstract: Two major challenges, high cost, and short lifespan, have been hindering the commercialization process of low-temperature fuel cells. Wei's group has been focusing on decreasing cathode Pt loadings without loss of activity and durability, and their research advances in this area over the past three decades are briefly reviewed herein. Regarding the Pt-based catalysts and the low Pt usage, they firstly tried to clarify the degradation mechanism of Pt/C catalysts and then demonstrated that the activity and stability could be improved by three strategies: regulating the nanostructures of the active sites, enhancing the effects of support materials, and optimizing structures of the three-phase boundary. For Pt-free catalysts, especially carbon-based ones, several strategies they proposed to enhance the activity of nitrogen-/heteroatom- doped carbon catalysts were firstly presented. Then, an in-depth understanding of the degradation mechanism for carbon-based catalysts was reported, followed by the corresponding stability enhancement strategies. Also, the carbon-based electrode at the micrometer-scale, faces the challenges such as low active-site density, thick catalytic layer, and the effect of hydrogen peroxide, which require rational structure design for the integral cathodic electrode. This review finally gave a short conclusion and outlook about the low cost and long lifespan of cathodic oxygen reduction catalysts.

Introduction

Low-temperature Fuel cells (FCs), as promising sources of power, can directly convert the chemical energy stored in hydrogen into electrical energy through electrochemical reactions. FCs have several benefits, such as zero emissions, high power density, low operating temperature, and fast response time, and they are being considered for use in various fields, including vehicles, submarines, and drones, etc. However, the current technical status suggests that in order to make fuel cell electric vehicles commercially viable, two major challenges need to be addressed: the high cost of FCs and their short lifespan when operating under vehicle conditions.

According to the U.S. Department of Energy 2020 indicator, low-temperature FCs require a Pt dosage of 0.125 $g \cdot kW^{-1}$. This means each automobile power fuel cell needs around 6.25 g (50kW) of Pt. In 2022, global automobile production reached about 85.02 million, which resulted in annual demand for Pt resources for onboard FCs of up to 531 tons. However, the current global annual production of Pt is only around 200 tons. The membrane electrode assembly (MEA) accounts for 84% of the fuel cell stack cost, with the cathodic and anodic electrodes containing Pt accounting for 54% of the MEA. Specifically, the slow oxygen reduction reaction (ORR) and the electrocatalysts' poor stability over time, particularly in corrosive environments, hinder the performance of the cathode in FCs. This is a significant obstacle to the widespread application of FCs on a large scale. In the field of electrocatalysts, it is essential to enhance the catalytic activity of ORR electrocatalysts to reduce the dependence on noble Pt or even to eliminate it completely. The crucial subject of electrocatalysts research is to find ways to decrease cathode Pt loadings without compromising on performance or durability, which can help in lowering the costs.

High-performance electrocatalysts for ORR require meeting certain fundamental requirements. These include high electrical conductivity, excellent catalytic activity, selectivity, and stability. The catalysts should possess high intrinsic electrical conductivity and efficient electron transfer capability. To ensure a high reaction kinetics, it needs the promotion of adsorption and activation of reactive species, orientation transformation of intermediate species, and timely desorption of products. Additionally, the catalyst must possess antioxidant, corrosion-resistant, and anti-poisoning properties under high electric field and impurity-containing reaction atmospheres. These properties ensure that the electrocatalytic reaction can be sustained and stabilized. The catalytic activity and antioxidant properties of the catalysts are closely linked to the adsorption strength of the catalyst and the intermediate species (oxygen-containing species). The corrosion resistance and anti-poisoning properties are closely related to the nature of the selected catalytic material and the selectivity of the species' adsorption. The catalytic performance of the catalyst is determined by both its geometrical and electronic structures. Therefore, ORR catalysts can be designed and optimized by adjusting their geometry and electronic structure.

To tackle the above issues, the Wei group from Chongqing University, China, has focused on screening the highly efficient ORR

electrocatalysts that do not contain Pt (Pt-free) or contain only a tiny amount of this noble metal (low-Pt) without compromising activity and durability. By addressing the underlying issues and core technical bottlenecks, they have been trying to gain an in-depth understanding of the electrocatalytic theory and the catalytic performance regulation mechanism for enhancing the activity and stability and have successfully developed a range of novel methods to prepare electrocatalysts with low cost, high activity, and superior stability.

1. Low Pt catalysts for ORR with high activity and stability

Reducing the amount of Pt while improving the activity and stability of the electrocatalyst is the key while challenging task in commercializing advanced energy conversion devices.[1, 2] In the past decades, extensive efforts have been contributed to promote the activity and stability of Pt-based nanoparticles (NPs, 2-5nm) catalysts.[3-6] The current state-of-the-art Pt-based catalysts have achieved satisfied catalytic activities that far exceed those of commercial Pt/C catalysts at the level of rotating disc electrodes in the laboratory. However, further pushing these catalysts with high activity and stability to produce impressive performance in practical MEAs has been difficult.[7-8] In FC operation, carbon-supported Pt-based NPs still suffer from serious corrosion of the carbon support, Pt dissolution, and Ostwald ripening. Unexpected power density losses in the mass transport region are observed in FCs with ultralow Pt loading (<0.1 mg·cm^{-2}). The development of highly dispersed catalysts with higher intrinsic activity and stability is extremely critical for achieving high current densities greater than 1.5 A·cm^{-2} in FCs.[9] In order to promote the development of low-Pt FCs, the Wei group deeply studied the degradation mechanism of Pt/C catalysts and proposed several efficient strategies to improve the catalytic activity and stability simultaneously, including regulating the Pt-based alloy structure, strengthening the metal-supported interaction, developing the new durable catalyst support, and optimizing the three-phase boundary in a catalytic layer.

1.1 Degradation mechanism of Pt/C catalysts

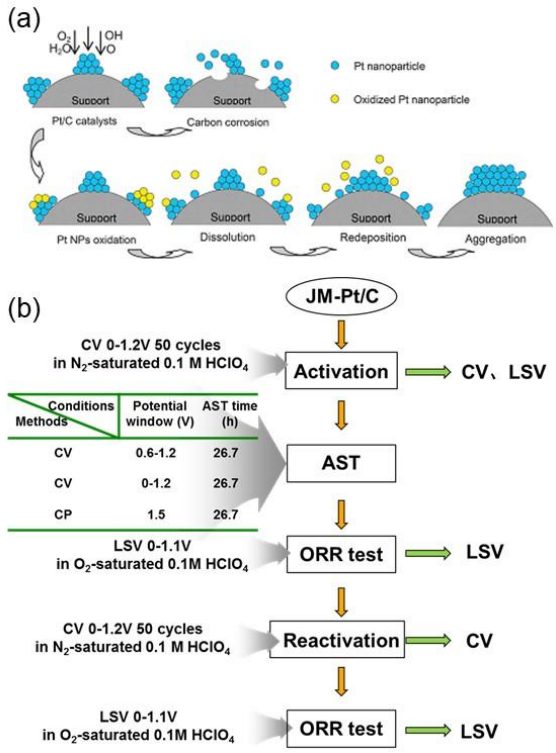

Figure 1. (a) Illustration of the degradation mechanism for the Pt/C catalysts[10]. Reproduced with permission of Ref. 10, copyright Springer Nature. (b) A combination method based on three different AST protocols.

For the past few decades, researchers have been working to study the degradation mechanism and improve the durability of Pt/C catalysts. The Pt/C catalysts degrade due to several mechanisms, as shown in Figure 1 a. Corrosion of the carbon support can lead to the detachment and aggregation of Pt NPs. The presence of H_2O_2 and O species during ORR can lead to the oxidation of Pt NPs, while smaller Pt particles are more likely to dissolve, then redeposit, and finally grow in size via Ostwald ripening and aggregation, causing significant loss of the Pt electrochemical surface area over time. All these factors contribute to the poor durability of the Pt/C catalysts.[10]

Accelerated stress tests (AST) are widely used to assess the long-term durability of FCs and their components. These tests include thermal degradation, reduced humidity, open circuit cell operation, and electrochemical forced aging under simulated cell conditions. The electrochemical forced aging includes potential cycling tests and potential holding tests. Different potential cycling

windows have been employed to evaluate the catalyst durability. Wei group proposed a combination method, as shown in Figure 1b, based on three different AST protocols to investigate the degradation mechanism of Pt/C catalysts[11]. They explored the degradation process of the catalyst under different electrochemical conditions and discovered that the formation of Pt oxide is a significant factor that affects the long-term stability of the catalyst. The loss of activity is categorized into two types: recoverable and unrecoverable. The former is caused by the reduction of Pt oxide or the removal of CO formed during carbon corrosion, while the latter is due to Pt dissolution/redeposition, agglomeration, detachment, and carbon corrosion. Using a more negative potential, the researchers are able to detect Pt dissolution/redeposition, while Pt agglomeration is found to be the main cause of Pt size growth. By monitoring the electrochemical impedance spectroscopy (EIS) response of the Pt catalyst under different potential windows, the researchers are able to identify the carbon corrosion mechanism. This test protocol is simple, efficient, and reliable and can be used to screen both new and existing electrocatalysts for FCs.

1.2 Structure regulating strategies for carbon-supported Pt-based alloy catalysts

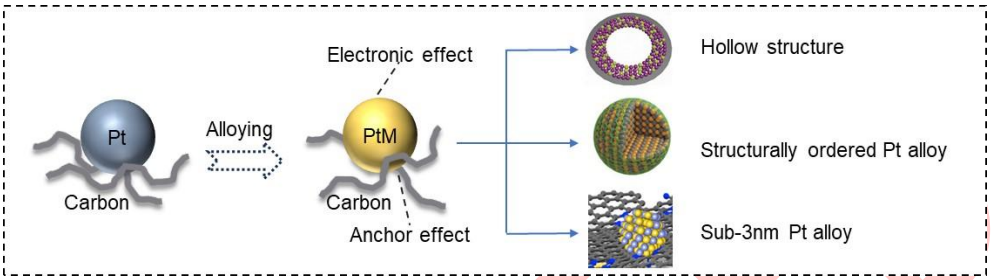

Figure 2. Schematic diagram of the strategies to enhance the performance of carbon-supported platinum-based alloy catalysts.

Carbon-supported Pt-based alloy catalysts with a lower Pt metal content exhibit not only the typical properties of phase pure Pt but also better performance compared to Pt/C catalysts. The modification of the surface electronic structure and the "anchor effect" of transition metal to Pt on the carbon surface are responsible for their increased activity and stability.[12] Generally, Pt-based alloys exhibit a down-shift d-band center, which weakens the adsorption strength of oxygen-containing species, thus allowing release of the active sites timely to increase the ORR activity. Furthermore, the "anchor effect" helps to alleviate the nanoparticles' sintering during the accelerated durability test at elevated temperature treatment. To develop high-performance low-Pt catalysts, the alloy structure should be designed to fulfill several conditions, including reduction of the Pt content, increase of Pt antioxidation ability, avoidance of the leaching of the transition metal, and optimization of the intrinsic activity. In Figure 2, strategies such as the formation of hollow structures, preparation of ordered intermetallic compounds, and synthesis of sub-3 nanometer alloy particles can fulfill the above demands as much as possible.

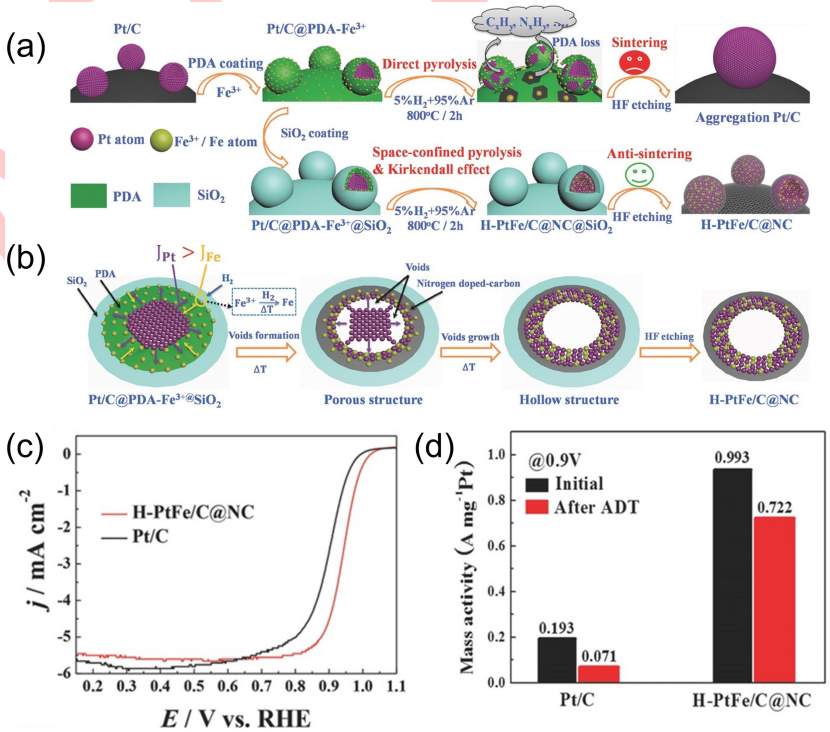

Figure 3. (a) and (b) Schematic fabrication of H-PtFe/C@NC. (c) ORR polarization curves of H-PtFe/C@NC and Pt/C catalysts recorded in RDE. (d) mass activity at 0.9 V versus reversible hydrogen electrode (RHE) for H-PtFe/C@NC and Pt/C catalysts before and after 20,000 potential cycles[13]. Reproduced with permission of Ref. 13, copyright John Wiley and Sons.

1.2.1 Hollow structure

The Pt-based hollow structures featuring high activity have been extensively investigated. The hollow structure of the catalysts significantly increases the number of available Pt atoms in the catalysts and further improves the performance of the catalysts through geometrical and coordination effects. However, conventional preparation methods do not allow economical commercialization of such hollow materials due to the barrier of high Gibbs formation energies. Wei group has developed a catalyst synthesis method based on space confinement and the Kirkendall effect in which a highly controlled transformation from solid Pt to hollow PtFe alloys under existence of suitably adsorbed Fe precursor is achieved[13]. In Figure 3, the hollow PtFe alloys featuring a Pt-skin can be directly transformed from solid Pt nanoparticles under space-confined conditions by H_2-assisted pyrolysis. Such spatially confined conditions include *in-situ* coating of commercial Pt/C surfaces with a layer of polydopamine, which has a very strong adsorption capacity for Fe^{3+}, followed by encapsulation with a silica layer. The high-temperature environment can provide high Gibbs formation energy and net atomic diffusion rate for formation of PtFe alloy catalysts. In the process of alloying, the PtFe alloy catalyst finally achieves a hollow structure due to the slower inward diffusion rate of the outer Fe atoms. Finally, after etching off the silica skin using HF, the nitrogen-doped carbon-shelled hollow PtFe alloy catalyst (H-PtFe/C@NC) was obtained. The prepared H-PtFe/C@NC exhibited significantly improved ORR activity (0.993 $A \cdot mg^{-1}_{Pt}$) compared to that of benchmark commercial Pt/C catalysts (0.193 $A \cdot mg^{-1}_{Pt}$). In addition to its high activity, H-PtFe/C@NC also exhibited high stability. After 20,000 cycles of cyclic potential scanning from 0.6 to 1.2 V in O_2-saturated 0.1 M $HClO_4$, the ORR half-wave potential of H-PtFe/C@NC shifted negatively by only 7 mV, and the mass-specific activity decreased by only 27.3% relative to the initial value. The H-PtFe/C@NC, after the stability test, still retained its original hollow structure, and no obvious particle agglomeration and size growth were observed. In contrast, the ORR half-wave potential of commercial Pt/C catalysts subjected to the same stability test conditions showed a negative shift of 49 mV and a 63.2% reduction in mass-specific activity.

1.2.2 Structurally ordered Pt alloy

Compared to disordered solid solution alloys, well-crystallized ordered intermetallic compounds, possess stronger interatomic interactions due to the ordered arrangement of metal atoms according to specific stoichiometric ratios. The formation of structurally ordered Pt-based alloys was demonstrated to be another effective strategy for mitigating the non-noble metal leaching and improving catalyst performance.[14,15] Wei group reported hollow and structurally ordered intermetallic PtFe alloy catalysts with over 6-fold enhancement in mass activity and specific activity relative to the pristine Pt/C catalyst.[16] The structural transformation dominated by the deposition and chemical ordering energies in the designed catalysts can be well tuned by precisely controlling the amount of adsorbed ions and the calcination temperature. In particular, the ordered PtFe alloy showed only 20.64% decrease in mass-specific activity after undergoing 3,000 cycles of potential scanning between 0.6 and 1.1V. The disordered PtFe alloy and Pt/C decay up to 42.59% and 62.79%, respectively, under the same accelerated stress test conditions. Similarly, an Au-stabilized $L1_0$-PtFe alloy catalyst was further prepared.[17] The formation of Au-Fe bonds in the catalyst suppressed the dissolution of Fe and modulated the electronic structure of Pt, thus endowing the catalyst with fantastic ORR activity and strong stability. Specifically, a mass activity up to 1.31 $A \cdot mg_{Pt}^{-1}$ was achieved by $L1_0$-PtAuFe, which was higher than that of $L1_0$-PtFe (1.26 $A \cdot mg_{Pt}^{-1}$) and commercial Pt/C (0.18 $A \cdot mg_{Pt}^{-1}$). More importantly, $L1_0$-PtAuFe showed a mass activity loss of only 30% after accelerated stress testing, which was significantly less than those of $L1_0$-PtFe (48%) and commercial Pt/C (63%).

1.2.3 Ultrafine intermetallic nanoparticles

Another way to reduce the use of expensive Pt in catalysis is to make the Pt-based alloy nanocrystals smaller, which increases the exposure of Pt atoms. However, obtaining sub-3 nm intermetallic Pt alloy nanocrystals for ORR without using confinement is difficult because the high temperature required for forming ordered intermetallic structures can cause the nanoparticles to clump together and grow in size. In Prof. Wei's early academic career, the particles of Pt or Pt alloys he prepared could reach as large as 22 nm even at a relatively low calcination temperature of 750 °C. [18] Later on, he tried to electrochemically deposit Pt and PtRu alloy uniformly on the porous carbon electrode in consideration of the atom-by-atom feature of metallic electrodeposting process. [19-24] Unfortunately, the precious metal atoms are more likely to deposit on themselves and on the sites where the electric field is stronger rather than to uniformly deposit on the whole carbon substrate regardless what deposition modulation condition was employed. This resulted in 5 ~ 8 nm Pt nanoparticles with uneven distribution on the carbon substrate as shown in the Figure 4a.

Fortunately, Wei and his coworker, Prof. Jing Li, teamed up to get out of the above dilemma. Recently, they reported a chemical bond weakening strategy for synthesizing carbon-supported sub-2 nm ordered intermetallic Pt alloy nanoclusters[25], as shown in Figure 4b. In the interdiffusion process in which two metal phases, Pt clusters and transition metal single-atom (MNC) with a common interface, are alloyed, introducing H_2 leads to spontaneous strong adsorption of H on Pt and N. The H_2 adsorption weakens and prolongs the bonds between Pt-Pt and M-N, thus increasing the mobility of atoms and reducing the kinetic barriers for forming Pt alloys with single M species. This results in the preparation of Pt alloys at a lower temperature, which inhibits the size growth and enables the formation of intermetallic nanocrystals like 1.55 nm Pt_3Fe and 1.25 nm Pt_3Ni. Both experimental and calculational studies confirmed a specific range of H_2 content (12-16 vol % H_2 in N_2) is necessary to form the Pt_3Fe-alloy phase, and that too much or too

little H_2 content does not allow formation of alloy, implying that the H_2 content plays a crucial role in this alloying process. By using an ultralow cathodic loading of 0.03 $mg_{Pt}·cm^{-2}$, an H_2-O_2 fuel cell assembled with Pt_3Ni cathode exhibits exceptional activity (1.60 $A·cm^{-2}$@0.67 V; 13.7 $W·mgPt^{-1}$ for the whole cell). After 100 hours of continuous operation under a potential of 0.6 V, a Pt_3Ni-based single cell shows a current-density decay of less than 3.7%, which suggests superior durability. This durability is attributed to the strong anchor of the Pt_3Ni nanoclusters on the graphene substrate.

High-entropy Pt alloy nanocrystals (HENs) with sub-3nm size are attracting increasing research interest for their advantage in modulating intrinsic activity and reducing Pt usage. While the present routes for preparing HENs, such as carbon-thermal-shock synthesis and wet chemistry method, cannot obtain effective size tuning and even dispersion of the nanocrystals, as well as their strong bonding on the carbon support at the same time. Interestingly, Wei group presented an anchoring-carbonization strategy for strongly bonding sub-3 nm HENs in ordered mesoporous carbon[26]. To the co-assembled system containing metallic species, carbon precursors, and the structure-directing agent F127, the first calcination in the mid-temperature region (< 400 °C) allows anchoring of the metal on the surface of partially carbonized phenolic resin skeleton as shown in Figure 4c. Then, at a higher temperature (~700 °C), a stronger planar contact rather than single point contact of HENs with carbon support was formed, which not only significantly suppressed the dissolution, migration, and agglomeration growth of HENs at high temperatures but also obtained a high-strength and stable anchoring of the HENs particles on the surface of the carbon support. Then, they were able to successfully incorporate different types of Pt-based HENs into porous carbon. The HENs had average nanocrystal sizes ranging from 2.2 to 2.9 nm for senary, septenary, octonary, and denary Pt-based HENs. ORR tests showed that the 6-HENs/PC (PtFeCoNiCuZn) catalyst had much better activity than low-entropy and medium-entropy alloy materials. This indicates that this approach has huge potential for producing efficient electrocatalysts. Additionally, the HENs were strongly anchored on the carbon support, which resulted in significantly higher electrochemical durability.

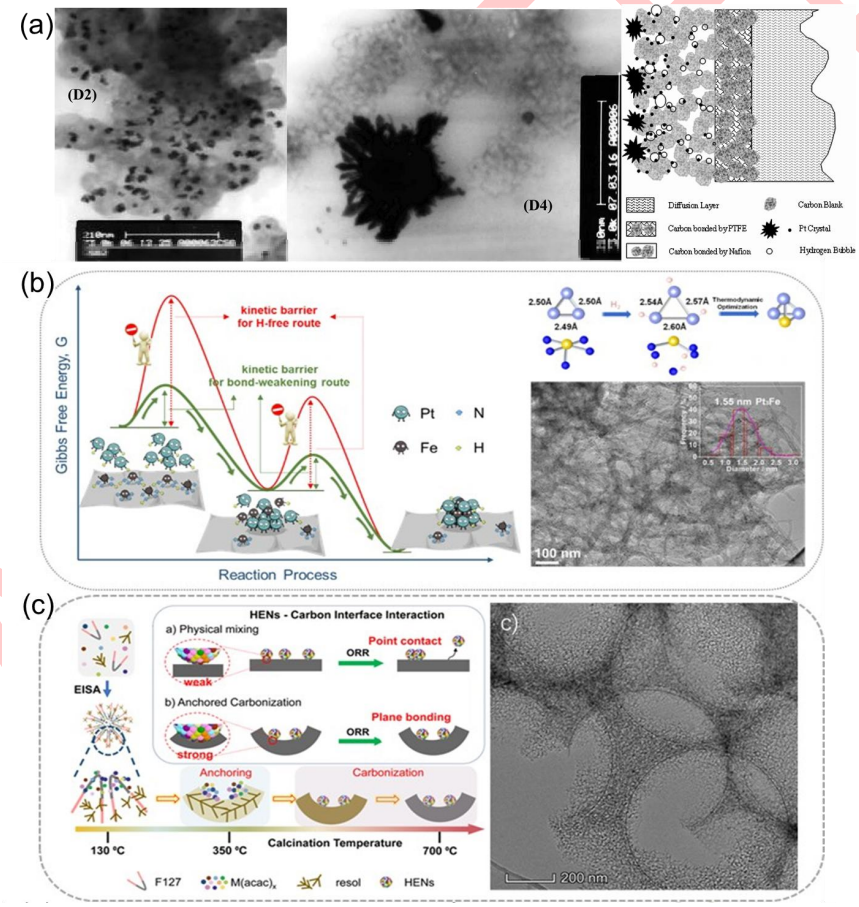

Figure 4. (a) Schematic illustration of the chemical bond-weakening strategy for preparation of Sub-2 nm intermetallic Pt alloy nanocrystals and the TEM image of Pt_3Fe/NC-500[23]. Reproduced with permission of Ref. 23, copyright Beijing Daxue Chubanshe.(b) Porous carbon supported sub-3 nm high-entropy Pt alloy nanocrystals. Schematic illustration of the HENs–carbon interfaces made by physical mixing and anchoring-carbonization strategy[25]. Reproduced with permission of Ref. 25, copyright Elsevier. (c) TEM image of 6-HENs/PC (PtFeCoNiCuZn) [26]. Reproduced with permission of Ref. 26, copyright John Wiley and Sons.

1.2.4 Multi-scale co-existing Pt catalysts

Since Prof. Tao Zhang and his coworkers first developed single-atom (SA) materials [27], SA catalysis has quickly become a research hotspot in the catalytic field. Recently, the SA catalysts with potential performance have been screened through first-principles machine learning methods [28]. The high catalytic performance of SA catalysts is attributed to their synergistic interaction

with ligand atoms and high atom utilization. Then, whether Pt, when prepared as single-atom catalysts, has the highest ORR activity and catalyst utilization. To answer this question, Wei's group conducted a comprehensive investigation to determine which is more effective for ORR - individual atoms, nanoclusters, or their coexistence. They investigated five catalysts: single-atomic Pt_{SA}/C, nanoclustered Pt_{NC}/C, and coexisted Pt_{SA-NC6}/C, $Pt_{SA-NC13}$/C, and $Pt_{SA-NC38}$/C.[29] Density functional theory (DFT) calculation results (Figure 5 a-b) show that at U = 0.9/1.23 V, Pt_{SA}/C has the highest reaction energy barrier in the initial O_2 adsorption step, while for Pt_{NC}/C, O_2 adsorption is spontaneous. Conversely, Pt_{NC}/C exhibits the rate-decisive step in the *OH desorption step, which is especially easy for Pt_{SA}/C. Particularly, for the three co-existed catalysts, the ΔG values for all steps are greatly decreased, indicating more easily happened ORR process. The in-depth analysis of the Bader charge well explains this. In Figure 5 c, SA has the largest Bader charge of 0.81, implying a significant electron loss of the Pt site, thus very weak adsorption to oxygen-containing species, by which the rate-decisive step is O_2 adsorption. In contrast, Pt_{NC}/C displays a Bader charge of −0.04, signifying a substantial electron gain, corresponding to too strong adsorption to oxygen intermediates, thus the desorption becomes the rate-decisive step. Interestingly, the three co-existed samples exhibit the moderate Bader charges of 0.73 ~ 0.78, well balancing the adsorption/desorption behavior for a more rapid $4e^-$ ORR kinetics. The experimental results well match with this DFT analysis. In H_2-O_2 MEA measurement, under an ultralow cathode Pt loading of 0.02 $mg_{Pt}\cdot cm^{-2}$, the coexisted Pt_{SA-NC} delivers a peak power density of 0.98 $W\cdot cm^{-2}$, being 2.3 times that of SA Pt, and 2.7 times that of Pt cluster-dominated catalyst.

The unsatisfactory physical and chemical stability of SA materials has heavily hindered practical applications in fuel cells. Recently, Shao and Wei reported a hybrid electrocatalyst consisting of highly dispersed Pt and Fe single atoms and PtFe alloy particles [30]. The prepared hybrid electrocatalyst had a size of 2~3nm and showed a mass activity of 0.77 $A\cdot mg^{-1}$ in the fuel cell, 3.7 times that of the commercial Pt/C catalysts. More impressively, due to the synergistic effect of the different active sites, the hybrid electrocatalyst showed negligible performance degradation at an ultra-low Pt loading of 0.015 $mg_{Pt}\cdot cm^{-2}$ in the cathode, even after 100,000 cycles harsh square-wave potential cycling or 200 h continuous operation at 0.6V. DFT calculations revealed that the synergistic Pt sites can accelerate the reaction step of oxygen-containing intermediates to water and reduce the accumulation of H_2O_2 in the electrode, thus reducing the degradation of components in the MEA and improving the durability of the electrode.

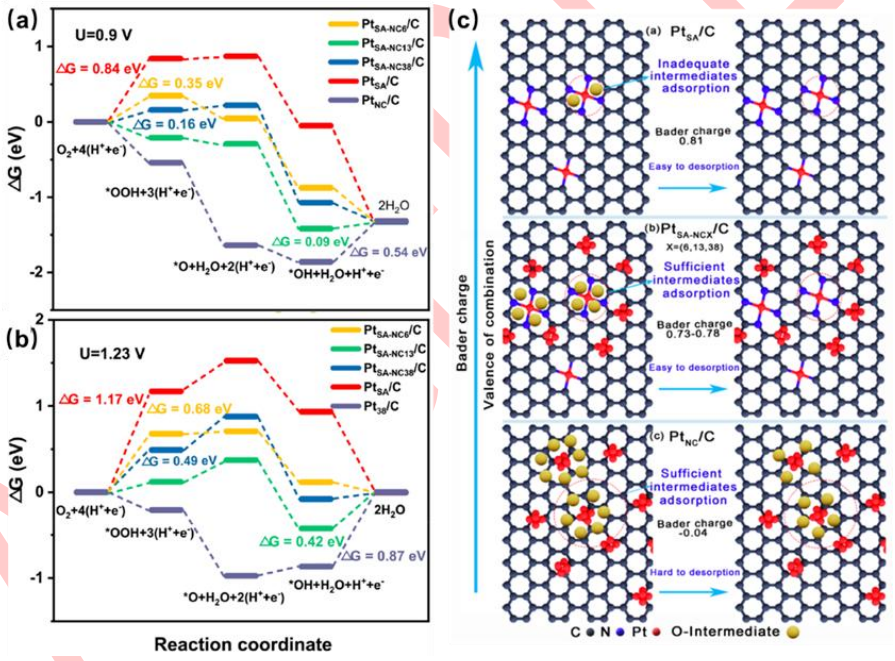

Figure 5. ORR free energy diagrams for the SA Pt, nanoclustered Pt, and the coexisted catalyst PtSA-NC at U= 0.9V (a) and 1.2 V (b) along ORR process; and (c) Bader charge analysis[29]. Reproduced with permission of Ref. 29, copyright American Chemical Society.

1.3 Supports enhancement mechanism for Pt-based catalysts

Having a good support is crucial as it not only prevents corrosion of the support itself but also helps in enhancing the Pt-support interaction strength and regulating the electronic structure of Pt-based alloys. It improves anti-oxidation ability of Pt NPs, inhibits the dissolution, migration, and aggregation of Pt NPs, and even enhances the intrinsic activity of catalysts. The most effective approaches to enhance the catalytic performance by tuning support include: forming functional coating on original support, modifying the supports, and replacing carbon black support with either more stable nanomaterials, such as carbon nanotubes (CNTs) and graphene, or non-carbon catalyst supports like transition metal oxides/nitrides, and MXene. As shown in Figure 6, all these methods increase the overlapping of orbitals between the support and Pt NPs and downshift the d-band center, leading to improved activity and stability.

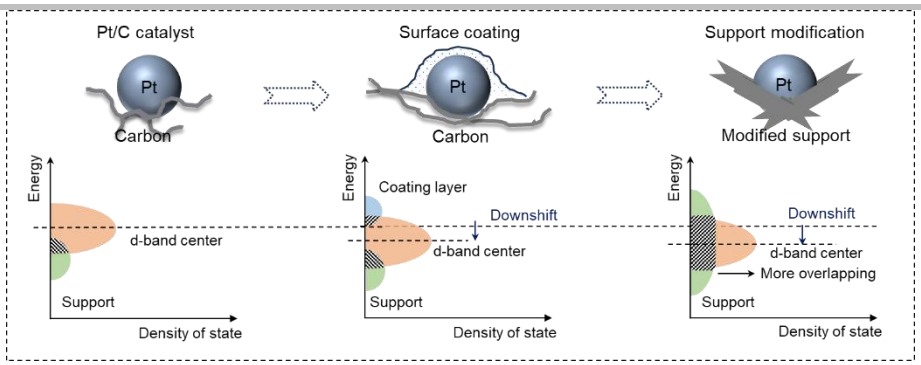

Figure 6. Schematic illustration of strategies and mechanisms for supports-enhanced performance of platinum-based catalysts

Wei group developed a method to coat carbon surfaces with a protector that can prevent direct exposure of the unstable carbon support to corrosive environments. In Figure 7, a core-shell catalyst, Pt/C@PANI, was designed and synthesized by polymerizing a thin layer of polyaniline (PANI) on the carbon surface of a Pt/C catalyst [31]. The stable PANI shell offers excellent environmental stability, high electrical and proton conductivity, unique redox properties, and acts as a protector for Pt/C catalyst, preventing direct contact of carbon support to corrosive environments. Moreover, the interaction between Pt NPs and the support is strengthened, which inhibits the agglomeration of Pt NPs. The charge transfer between PANI and Pt/C catalysts increases the conductivity of PANI and downshifts the d-band center of Pt, facilitating the desorption of oxygenate species, and enhancing the interaction between Pt NPs and the support [32]. The output performance of a fuel cell with Pt/C@PANI as the cathode catalyst only decreased by about 12% after 5,000 cycle stability tests at 0~1.2 V. In contrast, the output performance of the Pt/C fuel cell decreased by more than 85%. Furthermore, subjecting Pt/C@PANI to a high-temperature heat treatment could enhance the ORR activity. On the surface of Pt/C, the PANI undergoes *in-situ* conversion into highly graphitized GNC. The confinement effect of the PANI leads to the formation of Pt NPs with an anti-sinter capability. The size of Pt nanoparticles in Pt/C@NGC catalyst is only 4.7 nm even after a 900 °C heat treatment, as shown in Figure 7 e.

CNTs and graphene show potential as support materials for catalysts owing to their large surface area, high electrical conductivity, and excellent electrochemical durability. However, the surface of pristine CNTs and graphene is chemically inert, leading to relatively fewer binding sites for anchoring the Pt precursors or Pt NPs. This results in CNTs and graphene-supported catalysts having poor Pt dispersion and larger Pt NPs. Wei research group identified an organic functional group that could stabilize supported Pt NPs on CNTs. This functional group acts as a deposition and anchoring site for Pt NPs while simultaneously preserving the original structure of CNTs. Specifically, in Figure 8a and b, thiolate (-SH) groups are preferred as anchoring centers for Pt NPs compared to conventional hydroxylated and carboxylated groups. This is because the unoccupied d orbitals of the S atom are involved in hybridization and bonding, leading to an enhanced interaction between the Pt NPs and the CNT, restricting the migration of Pt on the CNT, and achieving a higher Pt dispersion. [26,33] The single-atom doped graphene can also exhibit a certain charge and increase catalyst activity by a coordination interaction such as electron transfer with other atoms. The merits of single-atom doped graphene support and Pt nanoparticles were combined by Wei group to prepare cross-linked multi-atom Pt catalysts for ORR (MAC-Pt/ZnFe-N-C, as shown in Figure 8 c.[34] The novel catalyst exposed 100% of the surface Pt atoms, yielding an impressive peak power density of 1.02 $W \cdot cm^{-2}$ in a real fuel cell at a low Pt loading of 35 $ug \cdot cm^{-2}$, almost twice that of a commercial Pt/C cell. In addition, the catalysts demonstrated excellent stability in both acidic and alkaline media, retaining 99.13 % and 98.40 % electrochemically active specific surface area (ECSA), respectively, after 2000 cycles of cyclic voltammograms.

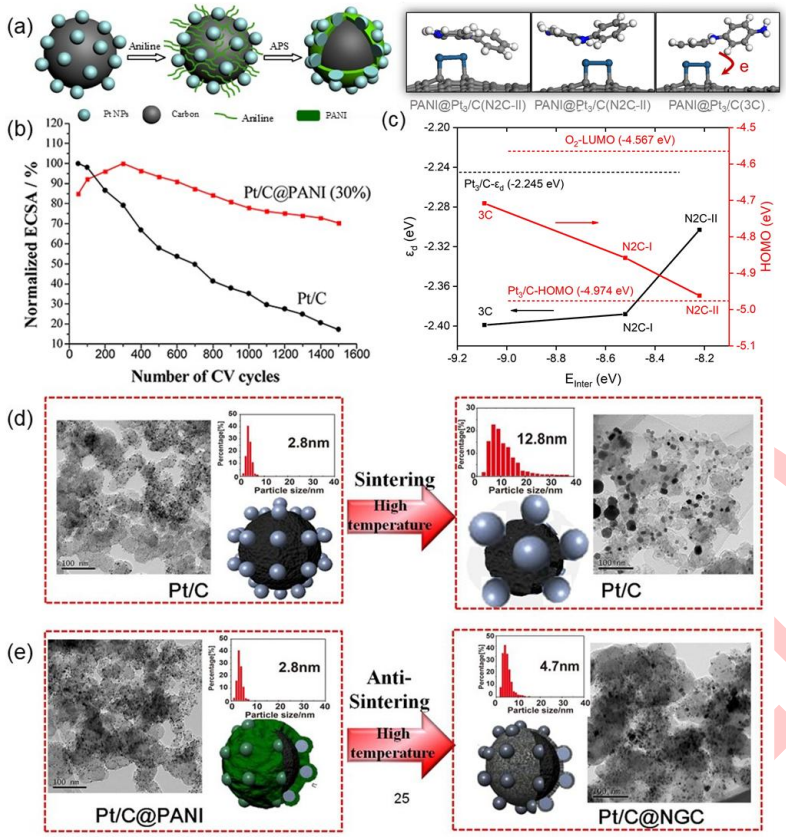

Figure 7. (a) Schematic of the preparation process of the Pt/C@PANI Catalyst. (b) ESCA retention of PANI@Pt/C (30%) and Pt/C catalysts. (c) The change of d band center and HOMO level of PANI@Pt/C models. TEM images of (d) fresh Pt/C catalyst and Pt/C catalyst after 1500 CV cycles, (e) fresh Pt/C@NGC catalyst and Pt/C@NGC catalyst after 1500 CV cycles[31]. Reproduced with permission of Ref. 31, copyright American Chemical Society.

Apart from the direct modulation of carbon-based supports, getting novel supports is also important for promoting the ORR performance of the catalysts. Wei group firstly adopted two-dimensional (2D) $Ti_3C_2X_2$ (X=OH, F) material as a novel alternative to conventional carbon support.[35] $Ti_3C_2X_2$ possesses outstanding functionalized surface properties, excellent conductivity, remarkable corrosion resistance, and robust anchorage to Pt NPs, rendering it a highly suitable catalyst support for FCs. Besides, as shown in Figure 8 d-e, the strong electron transfer caused by d orbits overlap for Pt and $Ti_3C_2X_2$ not only facilitates strongly anchoring of Pt nanoparticles on $Ti_3C_2X_2$ surface but also enhances the ORR activity [36]. The accelerated durability test confirmed that the $Ti_3C_2X_2$-supported Pt catalyst shows better stability than that of the commercial Pt/C catalyst, with no significant degradation observed in the Pt particle size and ORR half-wave potentials.

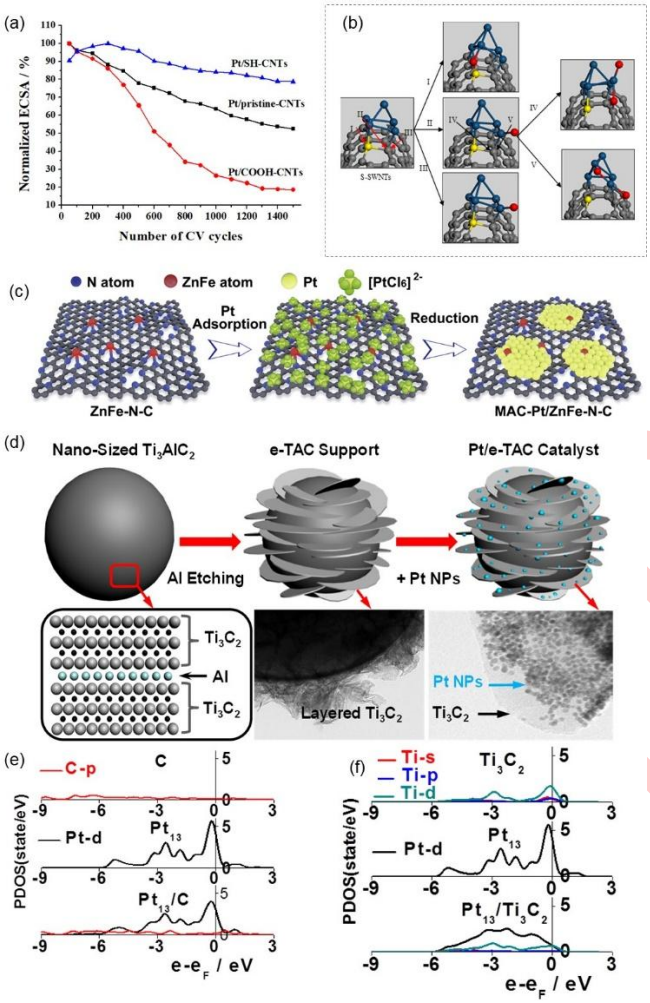

Figure 8. (a) Normalized Pt ECSA of electrodes made with Pt/SH-CNTs, Pt/pristine-CNTs and Pt/COOH-CNTs catalysts in N_2-purged 0.5 M H_2SO_4 at room temperature (0–1.2 V *vs.* RHE, sweep rate 50 mV s^{-1}) [24]. Reproduced with permission of Ref. 24, copyright Royal Society of Chemistry.(b) Attack configurations of O_{ad} on Pt_5/SH-SWCNTs[33]. Reproduced with permission of Ref. 33, copyright Royal Society of Chemistry.(c) Schematic illustration of the fabrication of MAC-Pt/ZnFe-N-C[34]. Reproduced with permission of Ref. 34, copyright Elsevier. (d) Schematic of Pt/e-TAC catalyst formation. The density of states for (e) Pt/C and (f) Pt/Ti_3C catalysts[36]. Reproduced with permission of Ref. 36, copyright Royal Society of Chemistry.

1.4 Optimizing strategies of three-phase boundary for Pt/C electrode

Apart from the electrocatalyst material, the catalyst layer in the cathode of MEA should also contain ionomer, electronic conductor (usually carbon) and gas and water transport channels, which can be summarized as "one reaction, two types of conductors, three-phase interface, and four kinds of channels" as shown in Figure 9. It means only the active sites which directly contact with both electron and ion conductors and locate just at the intersection of gas, liquid, electron, and proton transport channels, could participate in ORR. Thus the more such sites in the catalytic layer of the cathode, the better the MEA performance. The conventional catalytic layer is about 30-50 nm thick, in which randomly distributed catalyst particles and ionomers form many narrow channels and dead ends, which increase the gas-liquid diffusion resistance and even cause flooding by sacrificing gas transportation. Additionally, part of the Pt NPs embedded by carbon or ionomers cannot participate in the electrode reaction. Therefore, an improved electrode with proper gas transport, rapid water diffusion, and high electron and proton conductivity is urgently desired. Wei group developed an innovative method for preparing catalyst layers in FCs, known as alternative ion-exchange/electrodeposition (AIEE). [37] This method involves creating electronic and proton channels between Pt particles in the electrode and the current collector and electrolyte polymer, respectively. By constructing high Pt utilization electrodes in a solution that is free of Pt cations, the AIEE method significantly increases the utilization of Pt catalysts in the catalyst layer. The resulting MEA with a 0.014 $mg_{Pt}\,cm^{-2}$ AIEE electrode demonstrates a power output that is approximately 2.2 times larger than the one with a conventional Nafion-bonded electrode. This method ensures maximum exposure of the Pt particles to the three-phase zone, resulting in a more efficient fuel cell. Learned from the sophisticated brain neural system with the most efficient linkage, as shown in Figure 10, Wei group developed a bionic PtCo NPs network connected with carbon nanotube support to improve the overall Pt utilization in catalyst layer. [38] The bionic catalytic network is a highly effective system that enables the efficient transport of various species to active sites, resulting in a significant improvement in mass transfer efficiency compared to traditional Pt/C catalytic layers. This technology allows for a remarkable utilization efficiency of 58 $mg_{Pt}\cdot kW^{-1}$ in cathodes and 98 $mg_{Pt}\cdot kW^{-1}$ in both anodes and cathodes, almost three times

higher than traditional catalytic layers. Additionally, the bionic catalytic network-based fuel cell showed no decay during continuous operation at 1 A·cm^{-2} for 130 hours.

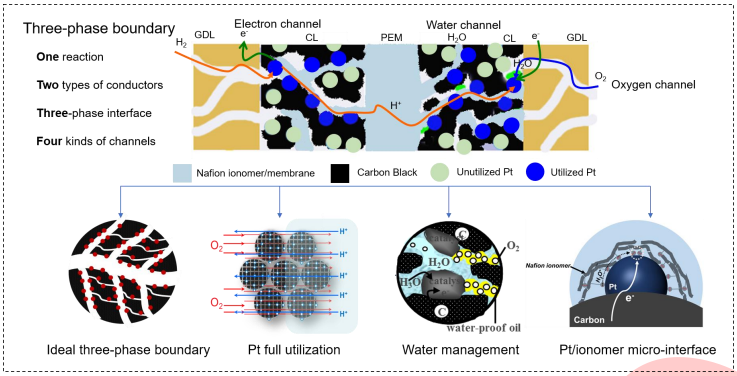

Figure 9. Schematic diagram of optimization strategy for the three-phase boundary of the porous electrode

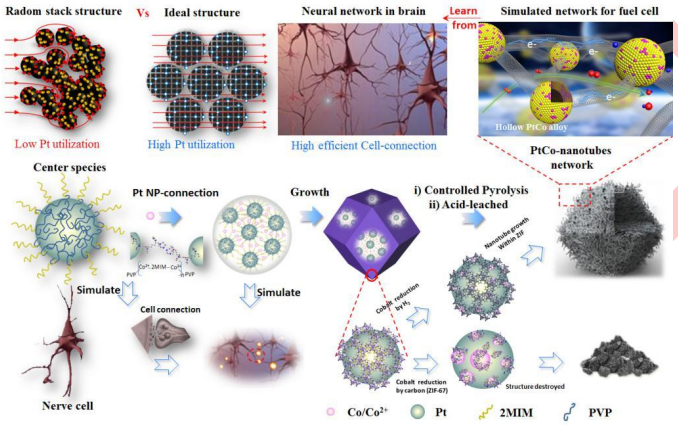

Figure 10. Schematic illustration of the bionic design of hollow alloy catalyst, inspired by nature (brain neural network) [38]. Reproduced with permission of Ref. 38, copyright Royal Society of Chemistry.

During the operation of FCs, the gas transport channel may be flooded with water due to the compressibility of the gas, a well-known "flooding" problem for the porous electrode. The main cause of the flooding is that the solubility of the non-polar O_2 molecule in the polar water molecules solvent is too low, and at the FCs operating temperature (60 ℃), the solubility of O_2 in the water will be further reduced due to the increase in vapor pressure of the water and the decrease in O_2 partial pressure. As a result, water gradually accumulates in the pores, especially with diameters ranging from 20 to 70 nm, due to capillary condensation that would not occur in the macro-pores. This makes it difficult to remove the water, thus exacerbating the flooding problem. Successfully solving the issue of water accumulation in these pores will be key to addressing the long-standing challenge of water management in FCs.

Wei group developed an "anti-flooding" strategy to modify the membrane electrode microchannels by preparing an anti-flooding electrode (AFE). [39-41] The strategy is based on the "principle of similar solubility" and involves adding a water-repellent and oxygen-rich oleophilic dimethylsiloxane (DMS) to the microchannels. The solubility of oxygen in the oxygen-rich oil phase is about 10 times higher than that in aqueous solution at room temperature. Moreover, the vapor pressure remains almost constant from 0 to 200°C, indicating that the solubility of oxygen doesn't change with temperature. When the fuel cell is operating at 80°C, the solubility of oxygen at that temperature is nearly zero due to the increase in water vapor pressure. However, the solubility of oxygen in DMS will be 61 times that in water, and considering the difference in diffusion coefficients of oxygen between the two, the transport of oxygen in DMS will be 28 times that in water. As shown in Figure 11, the waterproof oil occupies and modifies the pores of the microchannels, creating fixed transport channels for gases that are not flooded by water. This ensures the smooth and ordered fluid transport of "fish have fish channels; shrimp have shrimp channels." AFE prepared by adding DMS into a conventional porous electrode (CPE) showed an increase in the cell power from 1.01·W·cm^{-2} to 1.33·W·cm^{-2} under no humidification conditions, compared to that containing a CPE cathode. Additionally, the power output increased from 0.6 W·cm^{-2} to 1.2 W·cm^{-2} under over humidification conditions (156% RH). Furthermore, after over-humidification, CPE could only last for 3 hours of normal discharge, while AFE could last for 12 or 17 hours of normal discharge. The pore volume distribution analysis revealed that DMS mainly occupied the mesopores having diameters ranging from 20 to 70 nm. Particularly, the filled DMS would not be replaced by water due to the hydrophobic nature, which results in abundant transport channels being reserved for oxygen.

Wei group further proposed that the anti-flooding capability of the catalyst layer can be greatly improved by constructing hierarchically porous network without pores with diameters of 20-70 nm [42]. Using combined hard-soft template approach, the

ordered macro-mesoporous carbon-supported Pt nanocrystal catalyst was prepared which owns orderly arranged 500 nm macropores and 13 nm mesopores with 3 nm Pt nanoparticles uniformly distributed on the carbon surface. In Figure 12, the pore volume and the specific surface area of this porous catalyst are 3.4 and 4.5 times higher than those of the commercial Pt/C, respectively. With a quantitative evaluation using their self-designed “rattle-drum” like working electrode, the anti-flooding capability of the porous catalyst layer is almost 4 times higher than that constructed by commercial Pt/C. In the electrochemical test of the three-electrode system, the Pt/C electrode was instantly flooded, while the dual-porous electrode well remained continuous and stable running. The MEA test result shows that the peak power densities delivered by the porous electrode are 41% and 45% higher than those of Pt/C under typical and over-humidification test conditions, respectively. These results demonstrate that well-designed porous channels can significantly improve the mass transfer efficiency and anti-flooding capability of the catalyst layer for accelerated ORR kinetics.

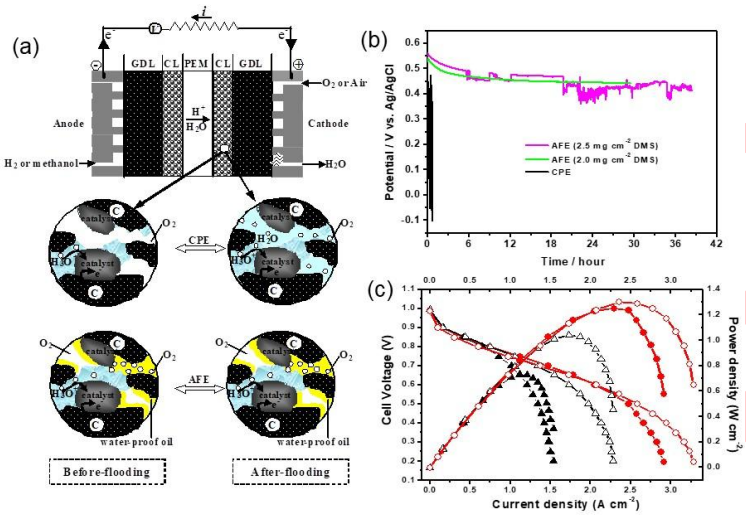

Figure 11. (a) Schematic of the water flooding in the CPE and AFE. (b) Cell voltage vs. Time of a MEA with an AFE or CPE as the cathode, and Cell voltage and Power density vs. current density of a single cell with a CPE anod and an AFE cathode in the case of no O_2 humidification (○) and O_2 over-humidification at 156% RH (●), and a single cell with two CPEs in the case of no O_2 humidification (Δ) and O_2 over-humidification at 156% RH (▲) [40]. Reproduced with permission of Ref. 40, copyright American Chemical Society.

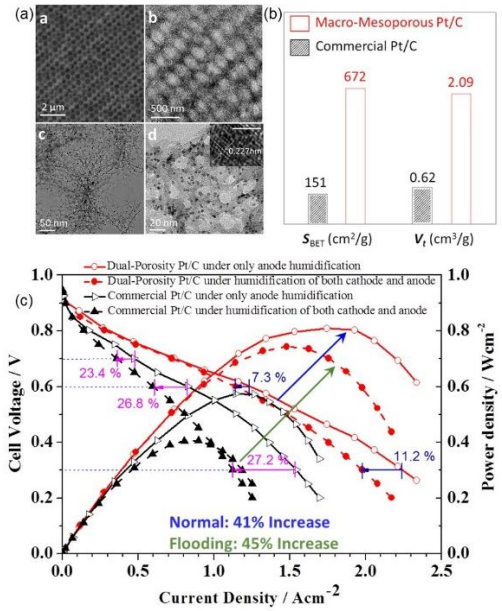

Figure 12. Anti-flooding catalyst layer constructed from ordered macro-mesoporous carbon. a) SEM and TEM images of the dual-porous carbon-supported Pt catalyst; b) comparison of the specific surface area and pore volume; c) MEA performance[42]. Reproduced with permission of Ref. 42, copyright John Wiley and Sons.

Perfluorinated sulfonic-acid ionomer is one of the most important components in FCs to provide proton transport channels. However, an increasing number of studies have shown that in conventional Pt catalyst layers, a thin layer of ionomers tightly covered

the surface of Pt particles, which led to the difficulty of oxygen diffusion toward the Pt sites. Also the specific adsorption of the sulfonate groups of the ionomers on the Pt surface suppressed its catalytic activity. It is important to note that highly active catalysts at the rotating disk electrode level frequently failed to exhibit excellent power density and stability in real FCs. Previous studies have revealed the importance of building effective Pt-ionomer interface in practical FCs. Wei group innovatively constructed a non-contact Pt/ionomer interface in the fuel cell catalyst layer by a blocking strategy.[43] They found that the hydroxyl group of cyclohexanol could be strongly coordinated to the sulfonate group of the ionomer, thus preventing the specific adsorption of the sulfonate group on the Pt surface, and mitigating the detrimental effects of the ionomer (Figure 13). The introduction of cyclohexanol resulted in a significant reduction in the coverage of sulfonate group on the Pt surface to ~7%, as compared to up to 21% coverage of sulfonate group in the conventional catalyst layer containing only Nafion ionomers. In the catalyst layer containing cyclohexanol, the coverage of the suppressed sulfonate group resulted in a 25% increase in the kinetic activity of the Pt at 0.85 V. Incorporation of cyclohexanol into the catalyst layer also increased the accessibility of oxygen and protons to the Pt surface, achieving a 24% enhancement of the peak power density in the mass transfer region of the H_2-air fuel cell.

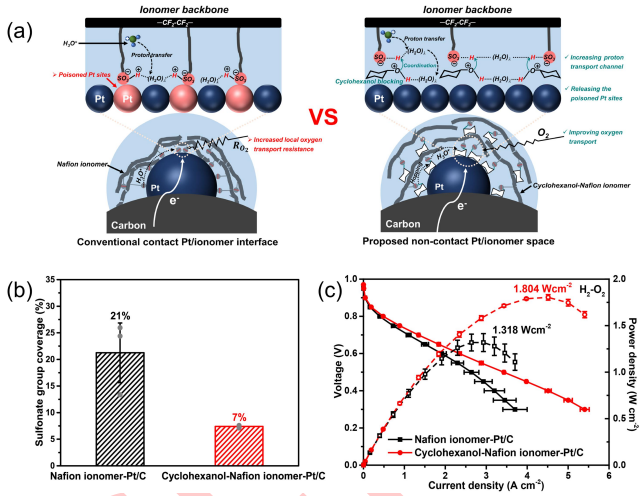

Figure 13. (a) Illustration of the conventional direct-contact Pt/ionomer interface and the proposed non-contact Pt/ionomer space for the cathode catalyst layer. (b) Sulfonate group coverage (in percent) for Nafion ionomer-Pt/C and cyclohexanol-Nafion ionomer-Pt/C. (c) H_2-O_2 fuel-cell performance of Nafion ionomer-Pt/C and cyclohexanol-Nafion ionomer-Pt/C catalyst layers[43]. Reproduced with permission of Ref. 43, copyright Springer Nature.

Catalyst poisoning is one of the most important problems leading to catalyst performance degradation. The poisoning of the kinetic activity of Pt catalysts by SO_x, CO and NO_x in air has been well known in practical low-temperature fuel cells. Wei's group investigated the effect of Mo atom doping on the SO_x resistance of Pt catalysts using DFT. [44] The results showed that Mo atoms weakened the S-Pt bond strength and mitigated the adsorption capacity of SO_x on the catalyst surface, which resulted in the electronic structure of PtMo (111) remaining unchanged after SO_x adsorption. In addition, they explored the CO tolerance of the Pt/WO_x@NC electrode.[45] The prepared electrodes showed excellent CO tolerance in liquid-phase tests with a CO electrooxidation potential of 0.24 V vs. RHE. More importantly, the Pt/WO_x@NC electrodes still showed a cell performance of about 133 mW·cm^{-2} even with a fuel containing 1000 ppm of CO, whereas the comparative Pt/C electrode with 100 ppm of CO completely lost its catalytic activity.

2. Carbon-based catalysts for ORR with high activity and stability

Carbon-based materials have gained widespread usage in the field of electrochemical energy due to their excellent physical properties, chemical stability, and electrical conductivity, along with being economical and easy to obtain. In particular, the gap between the initial performance of membrane electrodes assembled with carbon-based catalysts and that of Pt/C electrodes is decreasing, indicating the broad application prospect of such catalysts in FCs. Nonetheless, doped carbon-based catalysts still have many challenges under fuel cell operating conditions, such as low intrinsic activity, low activity density, and poor stability, which lead to too thick catalytic layer and fast degradation of initial battery performance. Over the past decade, Wei group[46-55] have extensively investigated the key scientific issues and core technical bottlenecks in carbon-based FCs. They have gained an in-depth understanding of the electrocatalytic theory and the catalytic performance regulation mechanism, which can significantly improve the performance and durability of non-precious metal carbon-based catalysts.

2.1 Strategies to increase the activity of nitrogen-doped carbon catalysts

Nitrogen-doped graphene (NG) carbon materials have been widely researched as potential catalysts due to their excellent ORR activity. NG carbon materials typically have three main nitrogen doping configurations - pyridine nitrogen, pyrrole nitrogen, and

quaternary nitrogen configurations, as shown in Figure 14. However, there has been a debate on which doping configuration has the higher ORR catalytic activity. Wei group[56,57] discovered that quaternary nitrogen is more favorable than in-plane NC (pyridine and pyrrole nitrogen) in terms of catalyzing the rate-determining step (RDS) of ORR, which is the protonation step of oxygen molecules. However, when the N-doped concentration is greater than 2.8 at%, the band gap of quaternary NC is significantly increased compared to planar NC, and the electron transport resistance becomes the determining step. Then, planar NC exhibits higher catalytic activity. The planar sp^2-hybridized N maintains the π-π conjugated structure of NC, which has more delocalized electrons and better electrical conductivity. On the contrary, the tetrahedral sp^3-hybridized N creates a steric structure for the NC, which has localized electrons and is not conducive to electron transfer. Literature analysis shows that all claims of high activity of quaternary NC have an N-doping concentration of less than 2.8 at%, and all claims of high activity of pyridine NC or pyrrole NC have an N-doping concentration of more than 2.8 at%, with few exceptions. This study convincingly identifies "which doping configuration has the highest ORR catalytic activity."

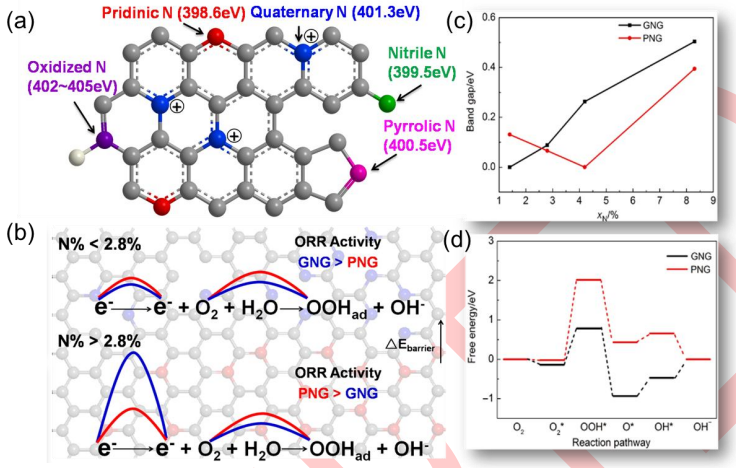

Figure 14. (a) Schematic representation of the common N bonding configurations[58]. Reproduced with permission of Ref. 58, copyright John Wiley and Sons. (b) a novel perspective about the dispute on the contribution of different N-type to ORR activity in N-doped graphene [56]. Reproduced with permission of Ref. 56, copyright Beijing Daxue Chubanshe. (c) Bandgap vs N doped content for GNG and PNG [57]. (d) Free energy curves of ORR on GNG and PNG [57]. Reproduced with permission of Ref. 57, copyright Beijing Daxue Chubanshe.

Based on the relationship among the nitrogen-doped configuration, the electric conductivity, and the ORR catalytic activity, Wei group[58] proposed the idea of spatial confinement-induced synthesis of planar nitrogen-doped carbons by selectively synthesizing planar pyridine- and pyrrolic-nitrogen-doped carbon materials with sp^2 hybrid orbitals, as shown in Figure 15. Layered montmorillonite (MMT) were used as a low-cost flat nanoreactor to selectively prepare planar NG nanosheets. The highest yield (90.3%) of planar NG was obtained using H-MMT with an interspace width of 0.46 nm. The quaternary and oxidized nitrogen content was restricted to less than 9.7% due to steric hindrance. The NG@MMT without metal exhibited excellent electronic conductivity and catalytic activity towards the ORR, making it a promising material for various applications. The single cell with the NG@MMT had a maximum power output of 320 mW·cm^{-2}, which was among the highest levels for similar materials achieved in 2013.

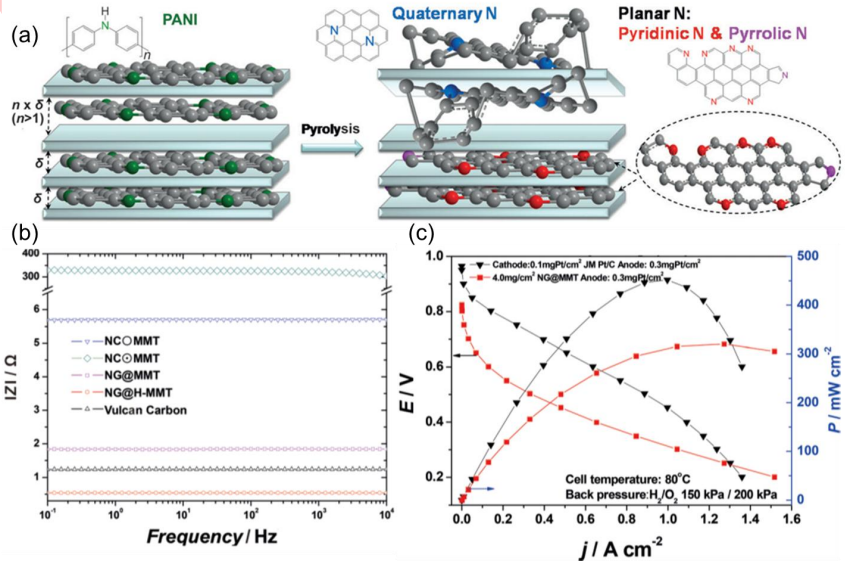

Figure 15. (a) Schematic representation showing the selectivity inside and outside of MMT during NG synthesis. (b) Bode spectra obtained through the application of a sine wave with an amplitude of 5.0 mV from 10 mHz to 10 kHz for different catalysts. (c) Polarization curves and corresponding power densities of membrane electrode assemblies fabricated with the NG@MMT cathode catalyst. [58] Reproduced with permission of Ref. 58, copyright John Wiley and Sons.

In order to enhance the performance of NC catalysts, it is crucial to increase the density of active sites and improve oxygen transport in the catalytic layer. However, the current density of exposed active sites, which are activated by planar pyridinic and pyrrolic N, is insufficient since they only appear at the edge of a large graphene sheet. To overcome this limitation, Wei group[59] developed a novel method called "shape fixing via salt recrystallization." This approach, shown in Figure 16, enables the efficient large-scale synthesis of N-doped carbon material with high ORR activity. The technique which envelops the nitrogen-containing polymer inside inorganic salt crystals via evaporative recrystallization of their mixed solution, results in four positive effects. Firstly, during the pyrolysis process that follows inorganic salt recrystallization, unpolymerized monomers, and solvent molecules become pore formers, causing the graphene to form inner pores, which results in a large number of inner edge pyridine and pyrrolic nitrogen-doped carbon. Secondly, the recrystallized inorganic salts stabilize the nanomorphology of nitrogen-containing polymers, maximizing the retention of the polymer's morphology at low temperatures in the final product after high-temperature carbonization. A favorable catalyst structure facilitates the availability of efficient mass-transport pathways and high utilization of active sites. Thirdly, the salt sealing effect of inorganic salt crystallization effectively resolves the problem of burn-off, high quaternary ammonia nitrogen doping, and structural collapse of the traditional direct carbonization method. Finally, this method overcomes the challenge of separating the template from the target catalyst, and it can be achieved solely by dissolving the cooled inorganic salt with water. The prepared N-doped catalysts exhibit outstanding ORR activity with a half-wave potential of only 58 mV behind that of Pt/C in an acidic medium. The PEMFC with the CPANI-Fe-NaCl-catalyzed cathode has a peak power output of 600 mW cm^{-2}, which is among the best for non-precious metal catalysts reported at the same period.

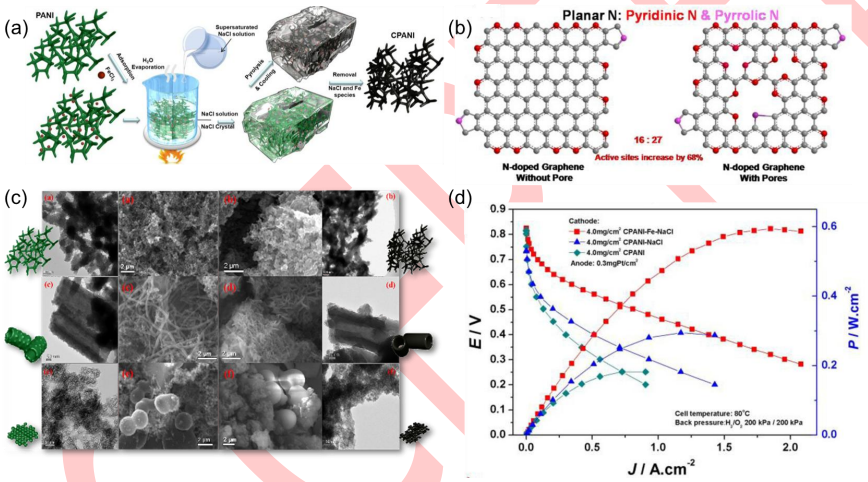

Figure 16. (a) Shape Fixing via Salt Recrystallization Method. (b) Schematic of active sites on edges and in pores. (c) TEM images of as-prepared materials and their carbonized products. (d) Polarization curves and corresponding power densities of membrane electrode assemblies fabricated with the CPANI-Fe-NaCl, CPANI-NaCl, and CPANI cathode catalysts[59]. Reproduced with permission of Ref. 59, copyright American Chemical Society.

2.2 Regulation mechanism of activity for heteroatom-doped carbon catalysts

Besides N, a plethora of other heteroatoms (e.g., N, B, O, P, S, Cl, Se, Br, and I) doped in graphene matrix has been reported as enhancing the catalytic activity of carbon-based catalysts. It led to ridicule from Professor Pumera's "Will Any Crap We Put into Graphene Increase Its Electrocatalytic Effect?" [60]. They demonstrated that bird dropping also can improve the electrocatalytic activity of graphene. This is indeed the case because the bird dropping contains nitrogen, uric acid, phosphoric acid, oxalic acid, and carbonate, which is rich in various heteroatoms such as N, P, S, and Cl. Bird-dropping-doped graphene coincided with heteroatoms-doped graphene. Despite this, it is still unclear which doping atom/group has the best effect on the ORR activity of graphene. It has been observed that positive charge doping caused by N and O being more electronegative than C, negative charge doping caused by B and P being less electronegative than C, or the doping of S and Se that have similar electronegativity to C without charge change, all enhance the activity of graphene. It is puzzling that it does not seem to matter whether the doping atom/group that enhances the activity is electron-donating or electron-withdrawing. Nonetheless, the catalytic regulation mechanism for heteroatom-doped carbon catalysts remains an area of active research and discovery.

In order to solve the problem mentioned above, Wei group[61,62] conducted a deep study on various heteroatom-doped carbon-based catalysts. They found that the intrinsic catalytic activity and ORR mechanism of doped-graphene catalysts were influenced by a triple effect, namely the charge, the spin density, and the coordinate state (ligand effect) of the carbon sites. In Figure 17, the effects that contribute to increasing the binding energies of *OOH or *OH can be ranked as follows: negative charge effect < positive charge effect < low spin effect < ligand effect < high spin effect. To improve the activity of graphene-based materials, a two-step strategy has been used in experiments by modifying the intrinsic electronic structure and increasing the defects. By combining these multiple effects, double active sites of carbon can be generated that catalyze ORR following the $4e^-$ dissociative mechanism. This strategy

overcomes the activity limitation of the associative mechanism and further enhances the catalytic activity for the ORR. Increasing the defects results in the output power of the nitrogen-doped carbon-based catalyst PEMFC increasing from 320 $mW \cdot cm^{-2}$ to 600 $mW \cdot cm^{-2}$. When S was additionally introduced into nitrogen-doped carbon to increase the spin density, the combination of spin and charge effect further increased the output power of PEMFC to 1100 $mW \cdot cm^{-2}$.

The synthesis of phosphorus-doped and nitrogen-phosphorus co-doped graphene has been achieved by utilizing the negative charge effect introduced by phosphorus doping and the positive and negative charge effect and ligand effect introduced by nitrogen and phosphorus co-doping[63,64]. These catalysts have been found to exhibit better activity for ORR in alkaline media compared to commercial Pt/C and RuO_2. In addition, the phosphorus-nitrogen co-doping enhances the anti-poisoning performance of carbon-based catalysts, which is particularly important for FCs operating in an atmospheric environment[65]. Catalysts on the cathode and anode of FCs are susceptible to degradation due to exposure to NOx and SOx in the atmosphere, as well as POx from high-temperature FCs membranes. Wei et al.[66] found that only proper P doping induces and promotes the incorporation of N atoms into the adjacent carbocycles, resulting in a P-C-N co-doped structure with an N/P ratio of 1:1, as shown in Figure 18. An excess of P can lead to the conversion of doped N from six-membered ring to five-membered ring, and P atoms are more inclined to combine with O to destroy the P-C-N co-doped structure. The P-C-N co-doped structure with an N/P ratio of 1:1 has been found to effectively eliminate the aggregation of toxic small molecules on the catalyst surface, making the concentration of NOx, SOx, and POx on the surface of PNC significantly lower than that of other catalysts, and showing excellent anti-poisoning performance.

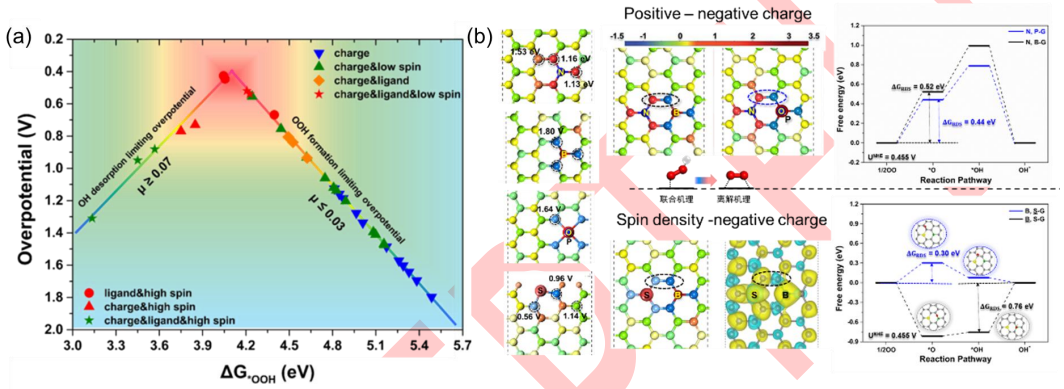

Figure 17. (a) The relationship of the ORR overpotential versus ΔG_{*OOH} for all the carbon active sites with joint participation of the charge, spin and ligand effects. The distribution of ΔG_{*OOH} for all the carbon active sites with separate participation of the charge effect; (b) Bader charge ,spin density distribution and free energy diagram of the ORR dissociative mechanism of the doped-G frameworks[61]. Reproduced with permission of Ref. 61, copyright Royal Society of Chemistry.

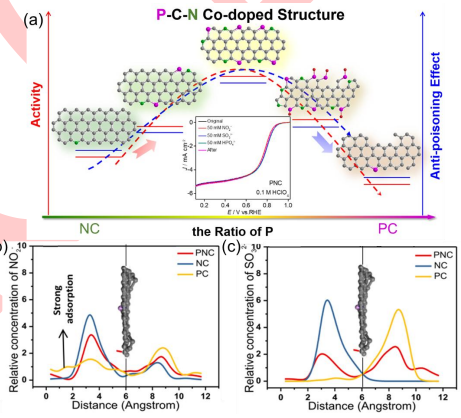

Figure 18. (a) Nitrogen-phosphorus double-doped carbon-based catalysts against NO_x and SO_x poisoning; (b-c) Relative concentration of NO_2^- and SO_3^{2-} along the z direction (perpendicular to the graphene surface) derived from MD simulation[66]. Reproduced with permission of Ref. 66, copyright John Wiley and Sons.

2.3 Degradation mechanism and stability enhancement for carbon-based catalysts

Carbon-based catalysts have become increasingly popular as alternatives to platinum-based catalysts in FCs due to their comparable activity levels. However, they still face significant challenges in terms of stability and durability under operating conditions, which have hindered their widespread application. One major issue is their rapid initial performance loss during stability testing, which greatly affects their performance. Various degradation mechanisms have been proposed for carbon-based catalysts during long-term fuel cell operation under dynamic load conditions, including nitrogen species protonation, carbon/metal oxidation, demetalation of metal atoms or active moieties, and water flooding. Moreover, abnormal operating conditions, such as insufficient air/fuel purging

during the shut-down/start-up process, can increase the cathodic potential to a higher level (1.5 V vs. RHE), adding to the complexity of the degradation process. During stability or durability testing, more than one of these degradation mechanisms may occur in parallel, making it challenging to identify the dominant one. Efforts are needed to develop strategies to enhance the stability and durability of carbon-based catalysts for their successful application in FCs.

During the process of ORR, it is relatively easier for nonmetallic atom doped-carbon-based catalysts to form surface oxidation intermediates (partial oxidation) on carbon sites rather than losing the carbon sites completely (complete oxidation) [67]. The interaction between carbon sites and oxygen species plays a crucial role in the formation of oxidation intermediates, while the loss of carbon sites is influenced by various factors such as oxidation intermediates, ORR mechanism, stability of the doped structure, and electrode potential. In situations where the associative or $2e^-$ ORR mechanism is involved, unstable doped structure, and high electrode potential, the partial or complete oxidation process can be expedited, as observed in P-G and Np-G cases. In P-G, the large atomic radius of P can lead to the loss of carbon sites and the formation of stable oxidation intermediates, which destroy the graphene structure. In Np-G, the relatively weak C-O binding energy can instigate the associative mechanism, which exacerbates the oxidation of carbon through the formation of *OOH. The ORR activity of doped graphene can be inhibited by both partial and complete oxidation of the carbon site.

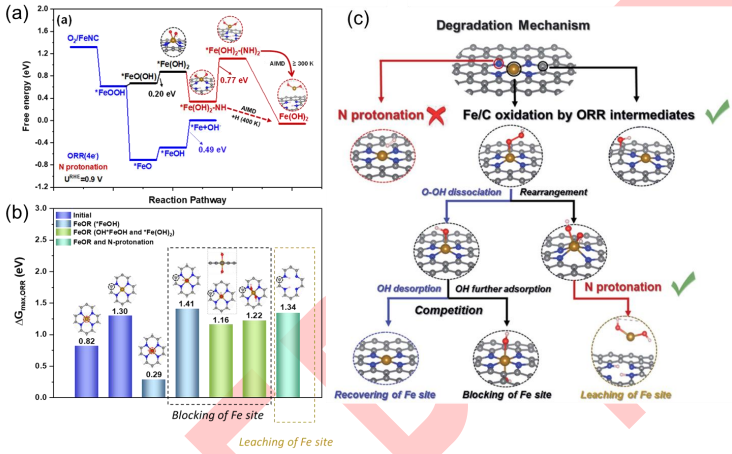

Figure 19. (a) The free energy diagram of FeOR at an electrode potential of U^{NHE} = 0.9 V involving ORR intermediates and an FeNC catalyst; (b) The maximum ΔG_{ORR} of active sites in different states; (a) The free energy diagram of FeOR at an electrode potential of U^{NHE} = 0.9 V involving ORR intermediates and an FeNC catalyst; (c) The pathway of the degradation mechanism of an FeNC catalyst[68]. Reproduced with permission of Ref. 68, copyright Royal Society of Chemistry.

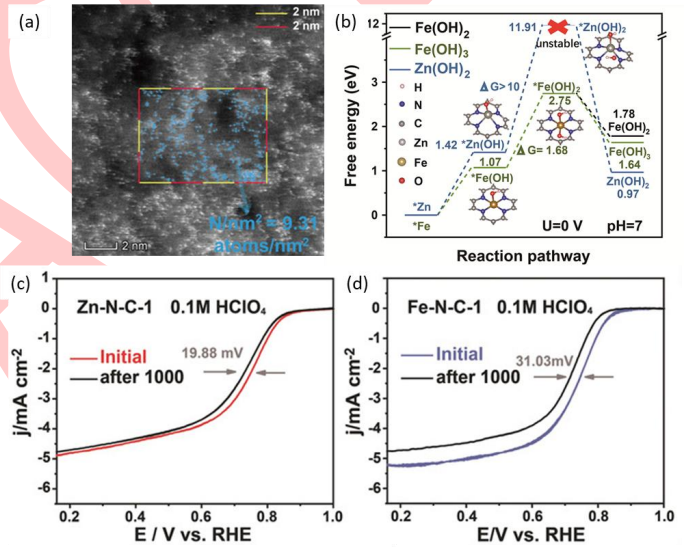

Figure 20. (a) HAADF-STEM image of the atomically dispersed Zn–N–C catalyst with an ultrahigh loading of single Zn atoms of 9.33 wt%; (b) Free-energy diagrams for $Zn(OH)_2$, $Fe(OH)_2$, and $Fe(OH)_3$ during the metal-corrosion process as based on the M–N_4 (M=Zn/Fe) structure; (c-d) ORR polarization of the Zn-N-C-1 and Fe-N-C-1 catalysts before and after 1000 cycles between 0.6 and 1.1 V versus RHE in 0.1 m $HClO_4$ solutions[69]. Reproduced with permission of Ref. 69, copyright John Wiley and Sons.

Wei group[68] further investigated the potential deactivation mechanisms of metal-doped carbon-based catalysts by using the FeN_4 moiety of FeNC catalysts as the active site model. They explored the critical factors for reversible and irreversible inactivation of the active sites of transitional metal-nitrogen-carbon (TMNC) catalysts (Figure 19). The N protonation of bare FeNC is difficult, while

Fe/C oxidation by ORR intermediates is inevitable. The occupation and recovery of Fe sites depend on the competition between adsorption and desorption of the intermediate species OH. When the adsorption and desorption are not in balance, the OH occupying the active site will hinder the progress of subsequent reactions, leading to reversible deactivation. Additionally, the rearrangement of OOH can cause asymmetric oxidation of the Fe site, weakening the Fe-N bond, triggering the protonation of N, and shedding and leaching of the active center in the form of $Fe(OH)_2$, resulting in irreversible inactivation. Meanwhile, based on the competition relationship between ORR and Fe oxidation, a trade-off potential was defined to evaluate the stability of the catalyst. The trade-off potential of FeNC (0.61 V vs. RHE) is much lower than the equilibrium (1.23 V) and half-wave potential (about 0.9 V) of ORR. Therefore, it is challenging for Fe sites to maintain the catalytic function of ORR in the working potential range, resulting in rapid activity attenuation. The more positive the value of the trade-off potential, the more difficult it is for the active site to be occupied by oxygen species, and thus, the less likely it is to be deactivated.

To overcome the intrinsic asymmetric oxidation of the FeNC catalyst, Wei group[69] successfully developed an ultrahigh-loading zinc single-atom catalyst. By controlling the doping and gasification process by decreasing the annealing rate to 1° min^{-1}, the Zn atoms can be embedded into the lattice of N-doped carbon substrate. The Zn atoms dispersed in the carbon substrate with an extremely high loading of 9.33 wt%, as shown in the HAADF-STEM image in Figure 20. The Zn-N-C catalyst was observed to be more stable than Fe-N-C. After AST of 1000 CV cycles between 0.6 and 1.1V in O_2-saturated 0.1 M $HClO_4$, Zn-N-C exhibited excellent stability of merely 19.88 mV decay of half-wave potential. The larger 31.03 mV decay of half-wave potential was observed for Fe-N-C. The high stability of Zn-N-C has been ascertained by theoretical calculation. The free energy required to form the asymmetric oxidation specie $*Zn(OH)_2$ is 11.91 eV, which induces a trade-off potential (1.24 V) of Zn-N-C to be higher than the equilibrium potential of ORR. This helps to avoid the protonation of nitrogen and imbalance of active site structure.

2.4 Rational construction of the carbon-based cathodic electrode

It is important to note that carbon-based catalysts in FCs still face many challenges, such as low activity and low active site density. To acquire enough active-site number in the MEA, such cheap catalysts normally require high loadings, which then results in thick catalytic layers of gas-porous electrodes. Additionally, there is a nonlinear coupling of heterogeneous transfer and electrochemical reaction within the thick catalytic layer. As a result, the efficiency of the porous electrode process decreases, leading to issues such as water flooding, uneven conductivity, and water vapor distribution. These issues can cause rapid battery performance decay. Moreover, the production of hydrogen peroxide caused by incomplete oxygen reduction can corrode carbon, membrane electrodes, and other materials of the battery system, which can lead to battery decay. Therefore, research on non-precious metal fuel cell catalysts should focus on improving the mass activity of carbon catalysts, fundamentally eliminating the generation of hydrogen peroxide, improving the global mass transfer efficiency in the catalytic layer, and enhancing the corrosion resistance and stability of the catalyst.[70-82]

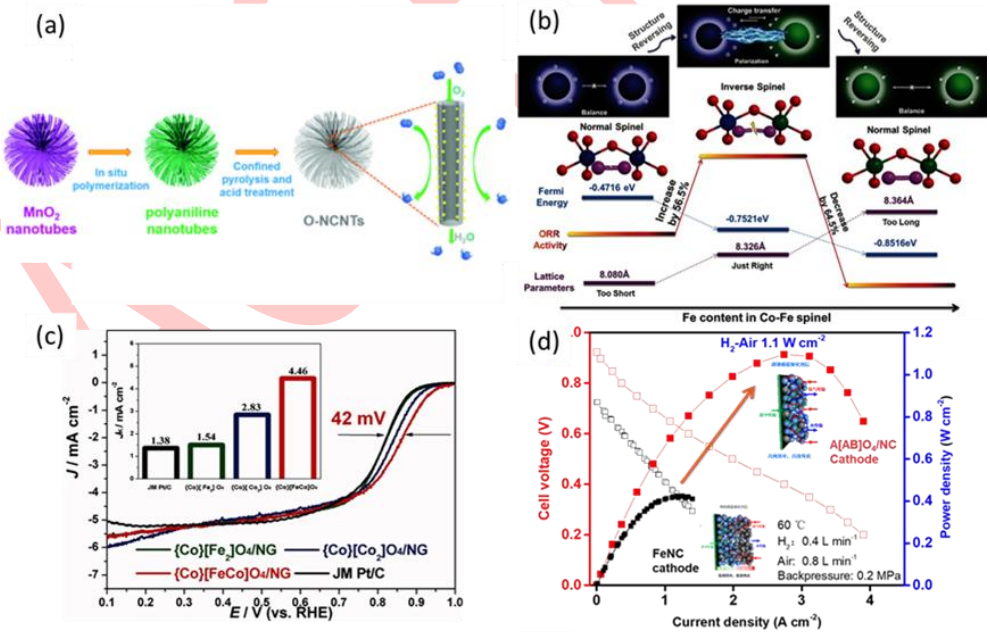

Figure 21. (a) Schematic illustration of the synthetic method for O-NCNTs based on the twice pseudomorphic transformation of MnO_2 nanotubes[85]. Reproduced with permission of Ref. 85, copyright Royal Society of Chemistry.(b) Representation showing the dissimilarity effect and polarization of octahedral atoms and the relationships between ORR activity and Fermi energy or lattice parameters (Fe green, Co blue, absorbed O magenta, lattice O red). (c) Linear sweep voltammetry (LSV) diagram of series of spinel catalyst and Pt/C[91]. Reproduced with permission of Ref. 91, copyright John Wiley and Sons.(d) Hydrogen-air non-precious metal fuel cell single cell with power exceeding 1.1W·cm^2.

3D porous structures have been found to offer significant advantages in improving the ORR activity of carbon materials by exposing more active sites and enhancing mass transport through forming mesopores and macrospores[83,84]. Wei group rationally

designed and controllably fabricated a porous nitrogen-doped carbon nanotube catalyst with open-ended channels for ORR (Figure 21a). [85] They achieved this by transforming MnO_2 nanotubes twice, which produced a highly defined structure with increased number of active sites for better performance. This catalyst facilitated both mass and electron transport, therefore leading to a significant increase in ORR activity. In comparison to the commonly used Pt/C catalysts, the O-NCNT catalysts showed superior ORR performance. Wei group[86] also employed SiO_2 microspheres as templates and fabricated several nitrogen-doped carbon catalysts with 3D hollow structures and controlled wall thickness. Thinner pore-walled catalysts outperform Pt/C catalysts in ORR due to their 3D hollow structure with a thin wall, leading to lower diffusion resistance and better mass diffusion. In order to fully utilize the active sites induced by nitrogen, a conductive backbone (CNT) has been adopted to eliminate the electron transport barrier of graphitic N in nitrogen-doped carbon. CNT@NC catalysts with a well-wrapped NC shell around a CNT core were prepared through a MnO_2 sacrificed-template method[87]. The CNT@NC showed better charge transfer properties compared to physically mixed NC+CNT and bulk NC, as evidenced by EIS. The increased conductivity of CNT@NC led to enhanced ORR activity, demonstrating the feasibility of the conductive backbone construction method for more effective active site utilization.

Combining carbon-based catalysts with transition metal compound catalysts can complement each other's strengths and weaknesses. This leads to enhanced intrinsic activity, density, and conductivity of the active sites. It also helps in reducing the formation of hydrogen peroxide, thereby improving the performance of cathodic porous electrodes. [88-90]. The ORR activity of spinel can be significantly improved by changing its crystalline structure from the normal to the inverse[91]. In Figure 21b, the inverse $[FeCo]O_4$ spinel exhibits the highest ORR activity among all spinel structures and exceeds that of the commercially available Pt/C by 42 mV in an alkaline medium. The dissimilarity effect of Fe and Co atoms at the octahedral sites modulates the activation energy and elongates O-O bonds compared to the normal spinel, resulting in enhanced intrinsic ORR activity on $[FeCo]O_4$. The combination of an ABO_3 catalyst with a NC catalyst eliminates the problem of mass transfer caused by insufficient active site density of carbon-based catalysts. This combination also promotes the decomposition of hydrogen peroxide intermediates generated by the ORR $2e^-$ mechanism on carbon-based catalysts. As a result, the active site density is increased, which further improves the catalytic activity of porous electrodes. In summary, porous electrodes assembled by the composite catalysts have achieved the present highest power density of H_2-air PEMFCs, which is 1.1 $W \cdot cm^{-2}$, and a performance of 360 $mA \cdot cm^{-2}$@800 mV, exceeding the DOE 2025 target of 300 $mA \cdot cm^{-2}$@800 mV.

Conclusion and outlook:

Pt-based electrocatalysts are known for their high and stable catalytic activity for ORR. However, the primary obstacle in the large-scale development of fuel cells (FCs) is the high cost of Pt, which needs to be reduced while improving the activity and stability during operating conditions. While low-cost carbon-based electrocatalysts can be used in FCs in large amounts, there is still a need to enhance their intrinsic activity, increase the active site density, and improve their stability to increase their durability under FC operating conditions. Aiming at the key scientific and technical issues behind FCs, Wei group carried out basic scientific research in order to improve the performance and durability of low-platinum and non-precious metal catalysts and has a deep understanding of the theoretical basis of electrocatalysis and catalyst regulation mechanisms. The mechanism and regulation strategy affecting the intrinsic performance of catalysts, together with the activity attenuation mechanism and stability enhancement mechanism of oxygen reduction catalysts, have been clearly detected. In addition, they put forward the important idea of reasonably preparing efficient gas porous electrodes and have successfully prepared a series of highly active and highly stable fuel cell cathode catalysts.

Developing new catalyst layers for ORR is closely linked to the creation of novel Pt-based and carbon-based catalyst systems that have improved intrinsic catalytic activity and better three-phase boundaries in MEA. Recent advances in catalyst exploration have led to some exciting developments in the understanding of the nature of catalysis, which allows for a more rational tuning of catalytic properties through controlled synthesis. By manipulating the surface chemisorption properties and altering the microscopic morphology and composition, highly active and stable Pt-based and carbon-based catalysts have been prepared. Loading these high-activity catalysts at the connection of electron, proton, gas, and water mass transport channels, and modulating the three-phase microenvironment can ensure the coupling of the reaction and mass transfer, prevent water flooding, and enhance the intrinsic activity and stability of catalysts. This can ensure the operational efficiency and stability of practical FCs. Although significant progress has been made in developing catalysts and interfacial structures for FCs, there are still major challenges to overcome in clean energy technologies. To improve the performance of ORR catalysts, it is important to focus on their intrinsic features such as shape, composition, and structure, as well as their interfacial/surface engineering. Additionally, understanding the arrangement of these catalysts, including the catalysts/ionomer interfacial structure, electrode/electrolyte/gas interface, within a real cell is crucial for a deeper understanding of the relationship between catalytic performance and catalyst structure.

In practical fuel cells, the cost, performance, and lifetime of the MEA are closely related to the nature of the catalyst. For Pt-based catalysts, challenges remain in further improving the intrinsic catalytic activity of the catalyst and optimizing the structure of the cathode catalyst layer. It needs to be recognized that carbon support is important for the performance of catalyst activity, even though the carbon support structure is difficult to tune due to its severely inhomogeneous properties. Further tuning of carbon support in terms of corrosion resistance, porosity, optimization of the Pt distribution position, as well as the use of functional group modification strategies are required to unlock the Pt catalyst performance further and improve stability. In practical catalytic layers, the importance of mass transport on electrode performance needs to be recognized. Structural strategies to design efficient mass transfer channels are necessary for electrode effectiveness, cost, and stability. The ionomer in the electrode is an important carrier for proton transport, but how to adjust its position, interactions, and dispersion to minimize the resistance to oxygen transport and inhibition of catalyst activity remains a focus of future research. In addition, machine learning methods provide opportunities and directions for finding next-generation catalysts as well as catalyst layers. For carbon-based electrocatalysts, there are still numerous challenges pertaining

to understanding the catalytic mechanism, regulating active sites, and developing highly efficient catalysts for practical applications in FCs. The active sites of carbon-based catalysts depend on the density of defect sites and the doped atoms, resulting in a large specific surface area needed and low active site density. In the catalytic layer, the number of active sites cannot be increased by increasing the amount of catalyst used, as this would result in a significantly elongated reactants and product mass transfer path. Therefore, the thickness of the carbon-based catalyst layer should be minimized as much as possible while providing sufficient activity. Furthermore, in addition to exploring methods to increase the stability of the catalyst itself, other methods, such as the addition of free radical quenching or trapping reagents, should be further developed.

Acknowledgments

This work was financially supported by the National Key Research and Development Program of China (No. (2020YFB1506002, 2019YFB1504503, 2016YFB0101202); National 973 Program of China (No. 2012CB215501); National Natural Science Foundation of China (No. 52021004, 22022502 (2021), 21822803(2019), 21576031 (2016), 51272297 (2013), 20936008(2010), 20676156(2007), 20376088(2004), 20176066(2002), 29976047(2000)).

References:

[1] Zheng Y, Petersen A S, Wan H, Hübner R, Zhang J, Wang J, Qi H, Ye Y, Liang C, Yang J, Cui Z, Meng Y, Zheng Z, Rossmeisl J, Liu W. Scalable and controllable synthesis of Pt-Ni bunched-nanocages aerogels as efficient electrocatalysts for oxygen reduction reaction [J]. Adv. Energy Mater., 2023, 13(20): 2204257-2204269.

[2] Zaman S, Su Y Q, Dong C L, Qi R, Huang L, Qin Y, Huang Y C, Li F M, You B, Guo W, Li Q, Ding S, Yu Xia B. Scalable molten salt synthesis of platinum alloys planted in metal-nitrogen-graphene for efficient oxygen reduction [J]. Angew. Chem. Int. Ed., 2022, 61(6): e202115835.

[3] Xiao F, Wang Q, Xu G L, Qin X, Hwang I, Sun C J, Liu M, Hua W, Wu H W, Zhu S, Li J C, Wang J G, Zhu Y M, Wu D J, Wei Z D, Gu M, Amine K, Shao M H. Atomically dispersed Pt and Fe sites and Pt-Fe nanoparticles for durable proton exchange membrane fuel cells [J]. Nat. Catal., 2022, 5(6): 503-512.

[4] Song T W, Xu C, Sheng Z T, Yan H K, Tong L, Liu J, Zeng W J, Zuo L J, Yin P, Zuo M, Chu S Q, Chen P, Liang H W. Small molecule-assisted synthesis of carbon supported platinum intermetallic fuel cell catalysts [J]. Nat. Commun., 2022, 13(1): 6521-6531.

[5] Liu J, Liu S, Yan F, Wen Z, Chen W, Liu X, Liu Q, Shang J, Yu R, Su D, Shui J. Ultrathin nanotube structure for mass-efficient and durable oxygen reduction reaction catalysts in PEM fuel cells [J]. J. Am. Chem. Soc., 2022, 144(41): 19106-19114.

[6] Hu Y, Zhu M, Luo X, Wu G, Chao T, Qu Y, Zhou F, Sun R, Han X, Li H, Jiang B, Wu Y, Hong X. Coplanar Pt/C nanomeshes with ultrastable oxygen reduction performance in fuel cells [J]. Angew. Chem. Int. Ed., 2021, 60(12): 6533-6538.

[7] Fan J, Wang H, Chen M, Zhao Z, Zhang Z, Ye S, L H. Bridging the gap between highly active oxygen reduction reaction catalysts and effective catalyst layers for proton exchange membrane fuel cells [J]. Nat. Energy, 2021, 6(5): 475-486.

[8] Kongkanand A, Mathias M F. The priority and challenge of high-power performance of low platinum proton-exchange membrane fuel cells [J]. J. Phys. Chem. Lett., 2016, 7(7): 1127-1137.

[9] Sievers G W, Jensen A W, Quinson J, Zana A, Bizzotto F, Oezaslan M, Dworzak A, Kirkensgaard J J K, Smitshuysen T E L, Kadkhodazadeh S, Juelsholt M, Jensen K M Ø, Anklam K, Wan H, Schäfer J, Čépe K, Escudero-Escribano M, Rossmeisl J, Quade A, Brüser V, Arenz M. Self-supported Pt-CoO networks combining high specific activity with high surface area for oxygen reduction [J]. Nat. Mater., 2021, 20(2): 208-213.

[10] Li L, Hu L P, Li J, Wei Z D. Enhanced stability of Pt nanoparticle electrocatalysts for fuel cells [J]. Nano Res., 2015, 8(2): 418-440.

[11] Zhang Y L, Chen S G, Wang Y, Ding W, Wu R, Li L, Qi X Q, Wei Z D. Study of the degradation mechanisms of carbon-supported platinum fuel cells catalyst via different accelerated stress test [J]. J. Power Sources, 2015, 273(1): 62-69.

[12] Wei Z D, Yin F, Li L L, Wei X W, Liu X A. Study of Pt/C and Pt-Fe/C catalysts for oxygen reduction in the light of quantum chemistry [J]. J. Electro. Chem., 2003, 541(1): 185-191.

[13] Wang Q M, Chen S G, Shi F, Chen K, Nie Y, Wang Y, Wu R, Li J, Zhang Y, Ding W, Li Y, Li L, Wei Z D. Structural evolution of solid Pt nanoparticles to a hollow PtFe alloy with a Pt-skin surface via space-confined pyrolysis and the nanoscale Kirkendall effect [J]. Adv. Mater., 2016, 28(48): 10673-10678.

[14] Wang Q M, Tang H, Wang M, Guo L, Chen S, Wei Z D. Precisely tuning the electronic structure of a structurally ordered PtCoFe alloy via a dual-component promoter strategy for oxygen reduction [J]. ChemComm., 2021, 57(33): 4047-4050.

[15] Gao X Y, Chen S G, Deng J H, Ibraheem S, Li J, Zhou Q Y, Lan H Y, Zou X, Wei Z D. High temperature self-assembly one-step synthesis of a structurally ordered PtFe catalyst for the oxygen reduction reaction [J]. ChemComm., 2019, 55(80): 12028-12031.

[16] Zou X, Chen S G, Wang Q M, Gao X Y, Li J, Li J, Li L, Ding W, Wei Z D. Leaching- and sintering-resistant hollow or structurally ordered intermetallic PtFe alloy catalysts for oxygen reduction reactions [J]. Nanoscale, 2019, 11(42): 20115-20122.

[17] Wang M J, Liu Y D, Li Y, Chen S G, Wei Z D. Stabilizing Fe in intermetallic $L1_0$-PtAuFe nanoparticles with strong Au-Fe bond to boost oxygen reduction reaction activity and durability [J]. Chem. Eng. J., 2023, 465(6): 142748.

[18] Wei Z D, Guo H T, Tang Z Y. Reduction of oxygen on a supported Pt-Fe-Co alloy catalyst with high surface area [J]. Chinese J. Catal., 1995, 16 (2): 141-144.

[19] Wei Z D, Chan S H, Li L L, et al. Electrodepositing Pt on a Nafion-bonded carbon electrode as a catalyzed electrode for oxygen reduction reaction [J]. Electrochim. Acta, 2005, 50(11): 2279-2287.

[20] Wei Z D, Chan S H. Electrochemical deposition of PtRu on an uncatalyzed carbon electrode for methanol electrooxidation [J]. J. Electroanal. Chem., 2004, 569(1): 23-33.

[21] Wei Z D, Li L L, Luo Y H, Yan C, Sun C X, Yin G Z, Shen P K. Electrooxidation of methanol on upd-Ru and upd-Sn modified Pt electrodes [J]. J. Phys. Chem.

B, 2006, 110(51): 26055-26061.
[22] Wei Z D, Chen S G, Liu Y, Sun C X, Shao Z G, Shen P K. Electrodepositing Pt by modulated pulse current on a nafion-bonded carbon substrate as an electrode for PEMFC [J]. J. Phys. Chem. C, 2007, 111(42): 15456-15463.
[23] Liu Y, Wei Z D, Chen S G, Feng Y C, Yin G Z, Sun C X. PEMFC electrodes platinized by modulated pulse current Electrodeposition [J]. Acta Physico-Chimica Sinica, 2007, 23(4): 521-525.
[24] Chen S, Wei Z, Guo L, Ding W, Dong L, Shen P, Qi X, Li L. Enhanced dispersion and durability of Pt nanoparticles on a thiolated CNT support [J]. ChemComm, 2011, 47(39): 10984-10986.
[25] Feng X, Yang N, Zhang W J, Hong W, Tan L Q, Wang F Z, Sun D, Ding W, Li J, Li L, Wei Z D. A sequential hydrogen-adsorption-assisted bond-weakening strategy for preparing sub-2-nm ordered Pt alloy nanocrystals [J]. Matter, 2022, 5(9): 2946-2959.
[26] Zhang W J, Feng X, Mao Z X, Li J, Wei Z D. Stably immobilizing sub-3 nm high-entropy Pt alloy nanocrystals in porous carbon as durable oxygen reduction electrocatalyst [J]. Adv. Funct. Mater., 2022, 32(44): 2204110-2204117.
[27] Qiao B, Wang A, Yang X, Allard L F, Jiang Z, Cui Y, Liu J, Zhang T. Single-atom catalysis of CO oxidation using Pt_1/FeO_x [J]. Nature Chem, 2011, 3(8): 634-641.
[28] Sun M Z, Huang B L. Direct Machine Learning Predictions of C3 Pathways [J]. Adv. Energy Mater., 2023, 2400152. DOI:10.1002/aenm.202400152
[29] Wang F Z, Yang J, Li J, Han Y Y, Li A, Xu R, Feng X, Wang T, Tong C, Li J W, Wei Z D. Which is Best for ORR: Single Atoms, Nanoclusters, or Coexistence? [J]. ACS Energy Lett., 2023, 9: 93-101.
[30] Xiao F, Wang Q, Xu L G, Qin X P, Hwang I H, Sun J C, Liu M, Hua W, Wu H W, Zhu S Q, Li J C, Wang J G, Zhun Y M, Wu D J, Wei Z D, Gu M, Amine K, Shao M H. Atomically dispersed Pt and Fe sites and Pt–Fe nanoparticles for durable proton exchange membrane fuel cells [J]. Nat Catal, 2022, 5: 503-512.
[31] Chen S G, Wei Z D, Qi X Q, Dong L C, Guo Y G, Wan L J, Shao Z G, Li L. Nanostructured polyaniline-decorated Pt/C@PANI core-shell catalyst with enhanced durability and activity [J]. J. Am. Chem. Soc., 2012, 134(32): 13252-13255.
[32] Wei Z D, Xue Y, Chen S, Li L, Xia M R. Density functional theory study of electronic structure and catalytic activity for Pt/C catalyst covered by polyaniline [J]. Sci. Sin. Chim., 2013, 43(11): 1566-1571.
[33] Li L, Chen S G, Wei Z D, Qi X Q, Xia M R, Wang Y Q. Experimental and DFT study of thiol-stabilized Pt/CNTs catalysts [J]. Phys. Chem. Chem. Phys., 2012, 14(48): 16581-16587.
[34] Li J, Zhou Q Y, Yue M F, Chen S G, Deng J H, Ping X Y, Li Y, Li J, Liao Q, Shao M H, Wei Z D. Cross-linked multi-atom Pt catalyst for highly efficient oxygen reduction catalysis [J]. Appl. Catal. B, 2021, 284(5): 119728.
[35] Xie X H, Chen S G, Ding W, Nie Y, Wei Z D. An extraordinarily stable catalyst: Pt NPs supported on two-dimensional $Ti_3C_2X_2$ (X = OH, F) nanosheets for oxygen reduction reaction [J]. ChemComm, 2013, 49(86): 10112-10114.
[36] Xie X H, Xue Y, Li L, Chen S G, Nie Y, Ding W, Wei Z D. Surface Al leached Ti_3AlC_2 as a substitute for carbon for use as a catalyst support in a harsh corrosive electrochemical system [J]. Nanoscale, 2014, 6(19): 11035-11040.
[37] Chen S G, Wei Z D, Li H, Li L. High Pt utilization PEMFC electrode obtained by alternative ion-exchange/electrodeposition [J]. ChemComm, 2010, 46(46): 8782-8784.
[38] Wang J, Wu G P, Wang W L, Xuan W H, Jiang J X, Wang J C, Li L, Lin W F, Ding W, Wei Z D. A neural-network-like catalyst structure for the oxygen reduction reaction: carbon nanotube bridged hollow PtCo alloy nanoparticles in a MOF-like matrix for energy technologies [J]. J. Mater. Chem. A., 2019, 7(34): 19786-19792.
[39] Ji M B, Wei Z D. A review of water management in polymer electrolyte membrane fuel cells [J]. Energies, 2009, 2(4): 1057-1106.
[40] Ji M B, Wei Z D, Chen S G, Li L. A novel antiflooding electrode for proton exchange membrane fuel cells [J]. J. Phys. Chem. C, 2009, 113(2): 765-771.
[41] Ji M B, Wei Z D, Chen S G, Qi X Q, Li L, Zhang Q, Liao C, Tang R. A novel anode for preventing liquid sealing effect in DMFC [J]. Int. J. Hydrogen Energy, 2009, 34(6): 2765-2770.
[42] Wang M J, Zhao T, Luo W, Mao Z X, Chen S, Ding W, Deng Y, Li W, Li J, Wei Z D. Quantified mass transfer and superior antiflooding performance of ordered macro-mesoporous electrocatalysts [J]. AIChE J., 2018, 64(7): 2881-2889.
[43] Chen F D, Chen S G, Wang A X, Wang M, Guo L, Wei Z D. Blocking the sulfonate group in Nafion to unlock platinum's activity in membrane electrode assemblies [J]. Nat. Catal., 2023, 6(5): 392-401.
[44] Xia M R, Liu Y, Li L, Xiong K, Qi X Q, Yang L J, Hu B S, Xue Y, Wei Z D. A DFT study on PtMo resistance to SO2 poisoning [J]. Sci. China Chem., 2013, 56(7): 1004-1008.
[45] Long D J, Ping X Y, Ni J T, Chen F D, Chen S G, Wei Z D, Guo L, Zheng J Y. Strengthening Pt/WO_x interfacial interactions to increase the CO tolerance of Pt for hydrogen oxidation reaction [J]. Chem. Commun., 2023, 59(91): 13583-13586.
[46] Zhang L, Li L, Chen H M, Wei Z D. Recent progress in precious metal-free carbon-based materials towards the oxygen reduction reaction: Activity, stability, and anti-poisoning [J]. Chem. Eur. J., 2020, 26(18): 3973-3990.
[47] Nie Y, Wei Z D. Electronic and physical property manipulations: Recent achievements towards heterogeneous carbon-based catalysts for oxygen reduction reaction [J]. ChemCatChem, 2019, 11(24): 5885-5897.
[48] Zhang W J, Li J, Wei Z D. Carbon-based catalysts of the oxygen reduction reaction: Mechanistic understanding and porous structures [J]. Chinese J. Catal., 2023, 48: 15-31.
[49] Wang Y, Huang X, Wei Z D. Recent developments in the use of single-atom catalysts for water splitting [J]. Chinese J. Catal., 2021, 42(8): 1269-1286.
[50] Peng L S, Wei Z D. Recent progress of mesoscience in design of electrocatalytic materials for hydrogen energy conversion [J]. Particuology 2020, 48: 19-33.
[51] Li J C, Wei Z, Liu D, Du D, Lin Y, Shao M. Dispersive single-atom metals anchored on functionalized nanocarbons for electrochemical reactions [J]. Electrocatalysis, 2020: 127-148.
[52] Xiao L, Yang Q Q, Wang M J, Mao Z X, Li J, Wei Z D. N-doped and Fe-, N-codoped carbon: tuning of porous structures for highly efficient oxygen reduction

reaction [J]. J. Mater. Sci., 2018, 53(21): 15246-15256.
[53] Wu R, Song Y J, Huang X, Chen S G, Ibraheem S, Deng J H, Li J, Qi X Q, Wei Z D. High-density active sites porous Fe/N/C electrocatalyst boosting the performance of proton exchange membrane fuel cells [J]. J. Power Sources, 2018, 401: 287-295.
[54] Wang Y, Li J, Wei Z D. Recent progress of carbon-based materials in oxygen reduction reaction catalysis [J]. ChemElectroChem, 2018, 5(14): 1764-1774.
[55] Wang Y, Chen W, Chen Y, Wei B, Chen L H, Peng L S, Xiang R, Li J, Wang Z C, Wei Z D. Carbon-based catalysts by structural manipulation with iron for oxygen reduction reaction [J]. J. Mater. Chem. A, 2018, 6 (18): 8405-8412.
[56] Wang J, Li L, Wei Z D. Density functional theory study of oxygen reduction reaction on different types of n-doped graphene [J]. Acta Phys. -Chim. Sin., 2016, 32(1): 321-328.
[57] Wang J, Wei Z D. Recent progress in non-precious metal catalysts for oxygen reduction reaction [J]. Acta Phys. -Chim. Sin., 2017, 33(5): 886-902.
[58] Ding W, Wei Z D, Chen S G, Qi X, Q Yang T, Hu J, Wang D, Wan L J, Alvi S F, Li L. Space-confinement-induced synthesis of pyridinic- and pyrrolic-nitrogen-doped graphene for the catalysis of oxygen reduction [J]. Angew. Chem. Int. Ed., 2013, 52(45): 11755-11759.
[59] Ding W, Li L, Xiong K, Wang Y, Li W, Nie Y, Chen S G, Qi X Q, Wei Z D. Shape fixing via salt recrystallization: A morphology-controlled approach to convert nanostructured polymer to carbon nanomaterial as a highly active catalyst for oxygen reduction reaction [J]. J. Am. Chem. Soc., 2015, 137(16): 5414-5420.
[60] Wang L, Sofer Z, Pumera M. Will any crap we put into graphene increase its electrocatalytic effect? [J]. ACS Nano, 2020, 14(1): 21-25.
[61] Yang N, Li L, Li J, Ding W, Wei Z D. Modulating the oxygen reduction activity of heteroatom-doped carbon catalysts via the triple effect: charge, spin density and ligand effect [J]. Chem. Sci., 2018, 9 (26): 5795-5804.
[62] Jiang S K, Zhang Z Y, Yang N, Li L, Wei Z D. Probing the interaction between nitrogen dopants and edge structures of doped graphene catalysts for the highly efficient oxygen reduction reaction [J]. J. Phys. Chem. C, 2022, 126(45): 19113-19121.
[63] Li R, Wei Z D, Gou X L. Nitrogen and phosphorus dual-doped graphene/carbon nanosheets as bifunctional electrocatalysts for oxygen reduction and evolution [J]. ACS Catal., 2015, 5(7): 4133-4142.
[64] Li R, Wei Z D, Gou X L, Xu W. Phosphorus-doped graphene nanosheets as efficient metal-free oxygen reduction electrocatalysts [J]. RSC Adv., 2013, 3(25): 9978-9984.
[65] Shah S S A, Najam T, Yang J, Javed M S, Peng L S, Wei Z D. Modulating the microenvironment structure of single zn atom: ZnN_4P/C active site for boosted oxygen reduction reaction [J]. Chinese J. Catal., 2022, 43(8): 2193-2201.
[66] Najam T, Shah S S A, Ding W, Jiang J, Jia L, Yao W, Li L, Wei Z D. An efficient anti-poisoning catalyst against SO_x, NO_x, and PO_x: P, N-doped carbon for oxygen reduction in acidic media [J]. Angew. Chem. Int. Ed., 2018, 130(46): 15321-15326.
[67] Yang N, Peng L L, Li L, Li J, Wei Z D. Theoretical research on the oxidation mechanism of doped carbon based catalysts for oxygen reduction reaction [J]. Phys. Chem. Chem. Phys., 2019, 21(47): 26102-26110.
[68] Yang N, Peng L L, Li L, Li J, Liao Q, Shao M H, Wei Z D. Theoretically probing the possible degradation mechanisms of an fenc catalyst during the oxygen reduction reaction [J]. Chem. Sci., 2021, 12(37): 12476-12484.
[69] Li J, Chen S G, Yang N, Deng M M, Ibraheem S, Deng J H, Li J, Li L, Wei Z D. Ultrahigh-loading zinc single-atom catalyst for highly efficient oxygen reduction in both acidic and alkaline media [J]. Angew. Chem. Int. Ed., 2019, 131(21): 7109-7113.
[70] Xiao F, Wang Y, Xu G L, Yang F, Zhu S, Sun C J, Cui Y, Xu Z, Zhao Q, Jang J. Fe-N-C boosts the stability of supported platinum nanoparticles for fuel cells [J]. J. Am. Chem. Soc., 2022, 144(44): 20372-20384.
[71] Xiao F, Liu X, Sun C J, Hwang I, Wang Q, Xu Z, Wang Y, Zhu S, Wu H W, Wei Z D. Solid-state synthesis of highly dispersed nitrogen-coordinated single iron atom electrocatalysts for proton exchange membrane fuel cells [J]. Nano Lett., 2021, 21(8): 3633-3639.
[72] He Q, Zeng L P, Wang J, Jiang J X, Zhang L, Wang J C, Ding W, Wei Z D. Polymer-coating-induced synthesis of FeN_x enriched carbon nanotubes as cathode that exceeds 1.0 W cm^{-2} peak power in both proton and anion exchange membrane fuel cells [J]. J. Power Sources, 2021, 489: 229499.
[73] Zhang Y D, Li J, Yang W, Zhang J, Fu Q, Song Y C, Wei Z D, Liao Q, Zhu X. Fe-N-doped carbon nanoparticles from coal tar soot and its novel application as a high performance air-cathode catalyst for microbial fuel cells [J]. Electrochim. Acta, 2020, 363: 137177.
[74] Mao Z X, Wang M J, Liu L, Peng L, Chen S G, Li L, Li J, Wei Z D. $ZnCl_2$ salt facilitated preparation of FeNC: Enhancing the content of active species and their exposure for highly-efficient oxygen reduction reaction [J]. Chinese J. Catal., 2020, 41(5): 799-806.
[75] Xi J Y, Meng K, Li Y, Wang M, Liao Q, Wei Z D, Shao M H, Wang J C. Performance improvement of ultra-low pt proton exchange membrane fuel cell by catalyst layer structure optimization [J]. Chin. J. Chem. Eng., 2022, 41: 473-479.
[76] Zhou Q Q, Li J, Yue M F, Wang M, Guo L, Li Y, Chen S G, Wei Z D. Maximizing metal utilization by coupling cross-linked ptru multi-atom on an atomically dispersed znfenc support [J]. Dalton Trans, 2021, 50(30): 10354-10358.
[77] Liu L H, Liu S, Li L, Qi H F, Yang H B, Huang Y Q, Wei Z D, Li L, Xu J M, Liu B. A general method to construct single-atom catalysts supported on n-doped graphene for energy applications [J]. J. Mater. Chem. A, 2020, 8(13): 6190-6195.
[78] Fan Z Y, Li J, Yang W, Fu Q, Sun K, Song Y C, Wei Z D, Liao Q, Zhu X. Green and facile synthesis of iron oxide nanoparticle-embedded N-doped biocarbon as an efficient oxygen reduction electrocatalyst for microbial fuel cells [J]. Chem. Eng. J., 2020, 385: 123393.
[79] Wu R, Wan X J, Deng J H, Huang X, Chen S G, Ding W, Li L, Liao Q, Wei Z D. NaCl protected synthesis of 3D hierarchical metal-free porous nitrogen-doped carbon catalysts for the oxygen reduction reaction in acidic electrolyte [J]. ChemComm, 2019, 55(61): 9023-9026.
[80] He Q, Chen X H, Jia F Q, Ding W, Zhou Y Y, Wang J, Song X Y, Jiang J X, Liao Q, Li J. The role of polyaniline molecular structure in producing high-performance Fe-N-C catalysts for oxygen reduction reaction [J]. ChemistrySelect, 2019, 4(27): 8135-8141.
[81] Shah S S A, Najam T, Cheng C, Peng L S, Xiang R, Zhang L, Deng J H, Ding W, Wei Z D. Exploring $Fe-N_x$ for peroxide reduction: Template-free synthesis of $Fe-N_x$ traumatized mesoporous carbon nanotubes as an orr catalyst in acidic and alkaline solutions [J]. Chem. Eur. J., 2018, 24(42): 10630-10635.
[82] Li J, Chen S G, Li W, Wu R, Ibraheem S, Li J, Ding W, Li L, Wei Z D. A eutectic salt-assisted semi-closed pyrolysis route to fabricate high-density active-site hierarchically porous Fe/N/C catalysts for the oxygen reduction reaction [J]. J. Mater. Chem. A, 2018, 6(32): 15504-15509.
[83] Li P B, Qi X Q, Zhao L, Wang J J, Wang M, Shao M H, Chen J S, Wu R, Wei Z D. Hierarchical 3D porous carbon with facilely accessible fe–n 4 single-atom

sites for Zn-air batteries [J]. J. Mater. Chem. A, 2022, 10(11): 5925-5929.

[84] Li J C, Cheng M, Li T, Ma L, Ruan X, Liu D, Cheng H M, Liu C, Du D, Wei Z D. Carbon nanotube-linked hollow carbon nanospheres doped with iron and nitrogen as single-atom catalysts for the oxygen reduction reaction in acidic solutions [J]. J. Mater. Chem. A, 2019, 7(24): 14478-14482.

[85] Wang Y, Chen W, Nie Y, Peng L S, Ding W, Chen S G, Li L, Wei Z D. Construction of a porous nitrogen-doped carbon nanotube with open-ended channels to effectively utilize the active sites for excellent oxygen reduction reaction activity [J]. ChemComm, 2017, 53(83): 11426-11429.

[86] Wu R, Wang J, Chen K, Chen S G, Li J, Wang Q, Nie Y, Song Y, Chen H, Wei Z D. Space-confined pyrolysis for the fabrication of fe/n/c nanoparticles as a high performance oxygen reduction reaction electrocatalyst [J]. Electrochim. Acta, 2017, 244: 47-53.

[87] Nie Y, Xie X H, Chen S G, Ding W, Qi X Q, Wang Y, Wang J, Li W, Wei Z D, Shao M H. Towards effective utilization of nitrogen-containing active sites: Nitrogen-doped carbon layers wrapped CNTs electrocatalysts for superior oxygen reduction [J]. Electrochim. Acta, 2016, 187: 153-160.

[88] Najam T, Shah S S A, Ding W, Ling Z, Li L, Wei Z D. Electron penetration from metal core to metal species attached skin in nitrogen-doped core-shell catalyst for enhancing oxygen evolution reaction [J]. Electrochim. Acta, 2019, 327: 134939.

[89] Wang Q M, Chen S G, Lan H Y, Li P, Ping X Y, Ibraheem S, Long D, Duan Y, Wei Z D. Thermally driven interfacial diffusion synthesis of nitrogen-doped carbon confined trimetallic Pt_3CoRu composites for the methanol oxidation reaction [J]. J. Mater. Chem. A, 2019, 7(30): 18143-18149.

[90] Ji D, Wang Y, Chen S G, Zhang Y L, Li L, Ding W, Wei Z D. Nitrogen-doped graphene wrapped around silver nanowires for enhanced catalysis in oxygen reduction reaction [J]. J Solid State Electrochem, 2018, 22(7): 2287-2296.

[91] Wu G P, Wang J, Ding W, Nie Y, Li L, Qi X Q, Chen S G, Wei Z D. A strategy to promote the electrocatalytic activity of spinels for oxygen reduction by structure reversal [J]. Angew. Chem. Int. Ed., 2016, 55(4): 1340-1344.

系列综述（1/4）:重庆大学魏子栋教授课题组在电化学能源转换方面的研究进展：燃料电池高性能氧还原催化剂

陈发东#，谢卓洋#，李孟婷，陈四国，丁炜，李莉*，李静*，魏子栋*

特种化学电源全国重点实验室（重庆大学），重庆大学化学化工学院

关键词：燃料电池，氧还原，铂基催化剂，碳基催化剂

摘要：燃料电池的规模化应用，尚需解决燃料电池成本高、工况下寿命短，以及核心材料电催化剂依赖进口等瓶颈和卡脖子问题。重庆大学魏子栋研究团队针对燃料电池面临的关键科学与技术问题，致力于开展提升燃料电池空气电极性能及低成本化的基础科学问题研究。本综述总结了该课题组过去三十年来围绕低铂和非贵碳基材料，提升空气电极活性与耐久性的研究进展。在铂基催化剂方面，首先阐述了 Pt/C 阴极催化剂的失活机制；总结了通过调节铂颗粒的纳米结构、修饰催化助剂、开发新型载体材料和精确调控三相界面微环境等，降低铂用量、提升电极性能和利用率的调控机制和制备策略。在非贵碳基催化剂方面，阐述了掺杂碳基催化剂氧还原活性的调节机制和失活机理；总结了致密活性位碳基催化剂结构调控、稳定性增强策略与绿色宏量可控制备策略。综述最后对低成本、长寿命燃料电池催化层结构优化与设计原则，以及面临的挑战进行了总结和展望。